

University of Windsor

Scholarship at UWindor

Electronic Theses and Dissertations

Theses, Dissertations, and Major Papers

10-5-2017

New ICE concept for hybrid application

WENZHOU LI

University of Windsor

Follow this and additional works at: <https://scholar.uwindsor.ca/etd>

Recommended Citation

LI, WENZHOU, "New ICE concept for hybrid application" (2017). *Electronic Theses and Dissertations*. 7273.

<https://scholar.uwindsor.ca/etd/7273>

This online database contains the full-text of PhD dissertations and Masters' theses of University of Windsor students from 1954 forward. These documents are made available for personal study and research purposes only, in accordance with the Canadian Copyright Act and the Creative Commons license—CC BY-NC-ND (Attribution, Non-Commercial, No Derivative Works). Under this license, works must always be attributed to the copyright holder (original author), cannot be used for any commercial purposes, and may not be altered. Any other use would require the permission of the copyright holder. Students may inquire about withdrawing their dissertation and/or thesis from this database. For additional inquiries, please contact the repository administrator via email (scholarship@uwindsor.ca) or by telephone at 519-253-3000ext. 3208.

New ICE concept for hybrid application
range extended series hybrid vehicle

by

Wenzhou Li

A Thesis
Submitted to the Faculty of Graduate Studies
through the Department of Mechanical, Automotive and Materials Engineering
in Partial Fulfillment of the Requirements for
the Degree of Master of Applied Science
at the University of Windsor

Windsor, Ontario, Canada

@2017 Wenzhou Li

New ICE concept for hybrid application
range extended series hybrid vehicle

by

Wenzhou Li

APPROVED BY:

P. Henshaw

Department of Civil and Environmental Engineering

A. Sobiesiak

Department of Mechanical, Automotive and Materials Engineering

D. Ting, Advisor

Department of Mechanical, Automotive and Materials Engineering

August 21, 2017

DECLARATION OF ORIGINALITY

I hereby certify that I am the sole author of this thesis and that no part of this thesis has been published or submitted for publication.

I certify that, to the best of my knowledge, my thesis does not infringe upon anyone's copyright nor violate any proprietary rights and that any ideas, techniques, quotations, or any other material from the work of other people included in my thesis, published or otherwise, are fully acknowledged in accordance with the standard referencing practices. Furthermore, to the extent that I have included copyrighted material that surpasses the bounds of fair dealing within the meaning of the Canada Copyright Act, I certify that I have obtained a written permission from the copyright owner(s) to include such material(s) in my thesis and have included copies of such copyright clearances to my appendix.

I declare that this is a true copy of my thesis, including any final revisions, as approved by my thesis committee and the Graduate Studies office, and that this thesis has not been submitted for a higher degree to any other University or Institution.

ABSTRACT

Due to increasingly strict regulations on automobile CO₂ emission around the world, this thesis focuses on the development of the control strategies of a plug-in series hybrid electric vehicle (HEV) with the goal of minimizing CO₂ emission. The thesis consists of three parts. The first target is to set up an electric vehicle (EV) model, which is the base of a plug-in series hybrid electric vehicle. The electric machine and battery are sized, and range capability and energy consumption are evaluated for a vehicle running in EV mode. The second objective is the assessment of the reference performance of the Range Extender (R-EX) architecture through the dynamic programming (DP) function in MATLAB, in terms of minimizing CO₂ emissions in the charge-sustaining condition. The third one is the development of the rule based control strategy through the analysis of the DP results by rules extraction.

In this thesis, a B-segment hatchback passenger car is modelled. The simulations were carried out along seven standard driving cycles that were developed to model different road conditions. This thesis also evaluates the effect of different values of auxiliary power on the electric range, energy consumption and thresholds of the rule-based control strategy. A sensitivity analysis of the carbon intensity of electricity is performed from a worldwide perspective.

Finally, the minimum values of CO₂ emission and the optimal engine operating points over different driving cycles are obtained from the dynamic programming; two flow charts of the proposed rule-based control strategies are derived, which are implementable for an electrical control unit to determine the power split between different energy sources.

DEDICATION

This thesis is dedicated to my family.

Only with their support,

I can face the difficulties encountered without their company.

TABLE OF CONTENTS

DECLARATION OF ORIGINALITY	III
ABSTRACT.....	IV
DEDICATION	V
LIST OF TABLES.....	VIII
LIST OF FIGURES.....	IX
LIST OF ABBREVIATIONS	XII
NOMENCLATURE.....	XIII
1 INTRODUCTION	1
1.1 MOTIVATION	1
1.2 HEV INTRODUCTION.....	2
1.3 RANGE EXTENDER.....	3
2 LITERATURE REVIEW	5
2.1 MODELLING METHODOLOGIES.....	5
2.1.1 Kinematic approach	5
2.1.2 Quasi static approach.....	6
2.1.3 Dynamic approach	7
2.2 CONTROL STRATEGIES	7
2.2.1 Offline Power Management Control Strategies.....	8
2.2.2 Online Power Management Control Strategies.....	8
2.2.3 Rule-based Power Management Control Strategies	9
2.2.4 Smart/ Learning Power Management Control Strategies [14].....	9
2.2.5 GPS enhanced Power Management Control Strategies [14]	9
3 CASE STUDY	11
3.1 VEHICLE MODELING	12
3.1.1 Electric Machine Model.....	13
3.1.2 Internal Combustion Engine Model.....	14
3.1.3 Battery Model	14
3.1.4 Braking system.....	15
3.2 OPERATING MODES	16
3.3 METHODOLOGY.....	16
3.3.1 DYNAMIC PROGRAMMING (DP)	17
3.3.2 RULE-BASED CONTROL STRATEGY	19

4 RESULTS	21
4.1 SIMULATION RESULTS (CHARGE DEPLETING CONDITION)	21
4.1.1 Sensitivity analysis.....	23
4.1.2 Performance Verification.....	26
4.2 SIMULATION RESULTS (CHARGE SUSTAINING CONDITION).....	26
4.2.1 WLTC	27
4.2.2 NEDC.....	30
4.2.3 US06	33
4.2.4 SCO3.....	35
4.2.5 NYCC	37
4.2.6 HWFET.....	39
4.2.7 FTP75.....	41
4.2.8 Summary of Driving cycles	43
4.2.9 Effect of Auxiliary Power.....	44
4.3 RULES EXTRACTION.....	47
4.3.1 Threshold of demand power	48
4.3.2 Threshold of vehicle speed	51
4.3.3 Threshold of vehicle acceleration	51
4.3.4 Proposed Rule-based Control Strategy	53
4.3.5 Effect of auxiliary power	54
5 CONCLUSIONS AND RECOMMENDATIONS.....	56
5.1 Conclusions.....	56
5.2 Recommendations.....	57
REFERENCES.....	59
APPENDIX.....	62
DRIVING CYCLES.....	62
VITA AUCTORIS	66

LIST OF TABLES

Table 1.1 CO ₂ emissions comparison among different kinds of vehicles [4].....	2
Table 3.1 Vehicle data	11
Table 3.2 RL coefficients for WLTC and NEDC	12
Table 4.1 Simulation results of NEDC and WLTC (TMH and TML)	22
Table 4.2 Simulation results of all the US driving cycles.....	23
Table 4.3 Electric range and energy consumption with the variation of auxiliary power ..	24
Table 4.4 CIE values for different areas in the year of 2011 [16]	25
Table 4.5 Results of CIE sensitivity analysis.....	25
Table 4.6 Acceleration time and maximum slope	26
Table 4.7 Results of CO ₂ production over different driving cycles	44
Table 4.8 Effect on CO ₂ production of adding auxiliary power of 500 W	44
Table 4.9 Effect on CO ₂ production of adding auxiliary power of 1000 W	45
Table 4.10 Effect on CO ₂ production of adding auxiliary power of 1500 W	45
Table 4.11 Effect on CO ₂ production of adding auxiliary power of 2000 W	46
Table 4.12 Mean value of demand power over different driving cycles	47
Table 4.13 Percentage of points outside the upper threshold for both EV and SERIES mode for different demand power.....	49
Table 4.14 Effect of auxiliary power on the thresholds.....	55

LIST OF FIGURES

Figure 1.1 CO ₂ emissions (g CO ₂ /km) normalized to NEDC [1].....	1
Figure 1.2 HEV classification.....	3
Figure 1.3 Range extender structure [7]	4
Figure 2.1 Information flow in a kinematic simulator (from Guzzella & Sciarretta 2007)..	5
Figure 2.2 Information flow in a backward model for motor vehicles fuel consumption calculation [11]	6
Figure 2.3 Information flow in a quasi-static powertrain model [11].....	7
Figure 3.1 Mechanical characteristic and efficiency map of the electric machines	13
Figure 3.2 Engine efficiency map with optimal operating line (OOL) and wide open throttle (WOT) line	14
Figure 3.3 R _{int} equivalent circuit model [31].....	15
Figure 3.4 Charge depleting and charge sustaining modes.....	16
Figure 3.5 Dynamic programming optimization	19
Figure 3.6 Example of rule-based control strategy [7]	20
Figure 4.1 Driving cycles for WLTC (left) and NEDC (right).....	21
Figure 4.2 Operating points in the EM efficiency map for WLTC (left) and NEDC (right)	21
Figure 4.3 Variation of battery SOC for WLTC (left) and NEDC (right).....	22
Figure 4.4 Electric range (left) and energy consumption (right) with the variation of auxiliary power	24
Figure 4.5 Results for demand power, EM power, ICE power, and battery power for WLTC	27
Figure 4.6 Optimal operating line and full load line for WLTC.....	28
Figure 4.7 Vehicle operating modes switching over WLTC	29
Figure 4.8 Vehicle operating modes switching over WLTC (point by point).....	30
Figure 4.9 Results for demand power, EM power, ICE power, and battery power for NEDC.....	31
Figure 4.10 Optimal operating line and full load line for NEDC	31
Figure 4.11 Vehicle operating modes switching over NEDC.....	32
Figure 4.12 Vehicle operating modes switching over NEDC (point by point)	32
Figure 4.13 Results for demand power, EM power, ICE power, and battery power for US06	33

Figure 4.14 Optimal operating line and full load line for US06 cycle	33
Figure 4.15 Vehicle operating modes switching over US06 cycle.....	34
Figure 4.16 Vehicle operating modes switching over US06 cycle (point by point).....	34
Figure 4.17 Results for demand power, EM power, ICE power, and battery power for SC03 cycle	35
Figure 4.18 Optimal operating line and full load line for SC03 cycle.....	35
Figure 4.19 Vehicle operating modes switching over SC03 cycle	36
Figure 4.20 Vehicle operating modes switching over SC03 cycle (point by point).....	36
Figure 4.21 Results for demand power, EM power, ICE power, and battery power for NYCC	37
Figure 4.22 Optimal operating line and full load line for NYCC	37
Figure 4.23 Vehicle operating modes switching over NYCC	38
Figure 4.24 Vehicle operating modes switching over NYCC (point by point)	38
Figure 4.25 Results for demand power, EM power, ICE power, and battery power for HWFET cycle	39
Figure 4.26 Optimal operating line and full load line for HWFET cycle.....	39
Figure 4.27 Vehicle operating modes switching over HWFET cycle	40
Figure 4.28 Vehicle operating modes switching over HWFET cycle (point by point)	40
Figure 4.29 Results for demand power, EM power, ICE power, and battery power for FTP75 cycle	41
Figure 4.30 Optimal operating line and full load line for FTP75 cycle.....	41
Figure 4.31 Vehicle operating modes switching over FTP75 cycle	42
Figure 4.32 Vehicle operating modes switching over FTP75 (point by point)	42
Figure 4.33 Variations of SOC along different driving cycles	43
Figure 4.34 Results of sensitivity analysis on CO ₂ emission.....	47
Figure 4.35 Number of points for EV and SERIES modes for each demand power.....	48
Figure 4.36 Upper threshold of demand power	49
Figure 4.37 Upper threshold verification for EV mode.....	50
Figure 4.38 Upper threshold verification for SERIES mode.....	50
Figure 4.39 Number of points for EV and SERIES modes for different vehicle speeds....	51
Figure 4.40 Number of points for EV and SERIES modes for each vehicle acceleration .	52
Figure 4.41 Upper threshold of vehicle acceleration	52
Figure 4.42 Upper Acceleration threshold verification for EV mode	53
Figure 4.43 Upper Acceleration threshold verification for SERIES mode	53

Figure 4.44 Rule-Based Control Strategy 54

LIST OF ABBREVIATIONS

Abbreviations

APU	Auxiliary Power Unit
CIE	Carbon Intensity of Electricity
DP	Dynamic Programming
ECMS	Equivalent Control Management Strategy
ECU	Electric Control Unit
EMS	Energy Management System
EV	Electric Vehicle
FTP75	Federal Test Procedure
HEV	Hybrid Electric Vehicle
HWFET	Highway Fuel Economy Driving Schedule
ICE	Internal Combustion Engine
NEDC	New European Driving Cycle
NYCC	New York City Cycle
OCV	Open Circuit Voltage
OOL	Optimal Operating Line
PHEV	Plug-in Hybrid Electric Vehicle
PMC	Power Management Control
R-EX	Range Extender
RL	Road Load
SC03	Supplemental Federal Test Procedure
SOC	State of Charge
TMH	Test Mass High
TML	Test Mass Low
WLTC	Worldwide Harmonized Light Vehicles Test Cycle
WOT	Wide Open Throttle

NOMENCLATURE

Symbols

Acc	Acceleration of the vehicle
a	Vehicle acceleration
C	Battery cell capacity
E_{batt}	Total electrical energy stored in the battery after recharging
$E_{consumed}$	Energy consumed over the simulation mission
EC	Energy consumption per one hundred kilometers
$F0$	Road load coefficient
$F1$	Road load coefficient
$F2$	Road load coefficient
F_{res}	Resistant force from the road
I	Battery cell current
i_g	Single speed transmission ratio
\dot{m}_f	Instantaneous fuel consumption of the engine
n	Number of cells in the battery pack
N_{max}	Maximum rotational speed of the electric motor
P_{AUX}	Auxiliary power
$P_{battery}$	Battery Power
P_{dmd}	Demand power from the road
P_{ICE}	Power of internal combustion engine
$P_{inertia}$	Inertia Power due to vehicle acceleration
P_{em}	Power of electric motor
P_{GEN}	Power of generator
P_{res}	Resistant power from the road
$P_{traction}$	Traction Power
$R_{h,parallel}$	Hybridization Ratio of parallel hybrid electric vehicle
$R_{h,SERIES}$	Hybridization Ratio of series hybrid electric vehicle
$R0$	Internal Resistance
R_{wheel}	Radius of wheel
SOC_{END}	Final value of SOC at the end of simulation mission
T	Duration of the vehicle mission
T_{wheel}	Torque on the wheel

t	Acceleration time
$u(t)$	Vector of the control variables
v	Vehicle speed
V	Battery cell voltage
v_{max}	Maximum vehicle speed
π	PI coefficient
δ	Mass factor considering the inertia values of rotating parts
$\eta_{gearbox}$	Gearbox efficiency
$\eta_{electric\ generator}$	Electric generator efficiency
μ_{CO_2}	Molar mass of CO ₂
μ_{fuel}	Molar mass of fuel
ΔSOC	Variation of the state of charge
Δt	Time interval
α	Maximum slope the vehicle is able to overcome

1 INTRODUCTION

1.1 Motivation

To address environmental concerns, the regulations of automobile emissions are becoming increasingly strict around the world. With regard to mitigating greenhouse effects, the reduction of CO₂ emission is the main challenge for automobile manufacturers, Figure 1.1 [1] presents the global trend of automotive CO₂ emission from 2000 to 2025.

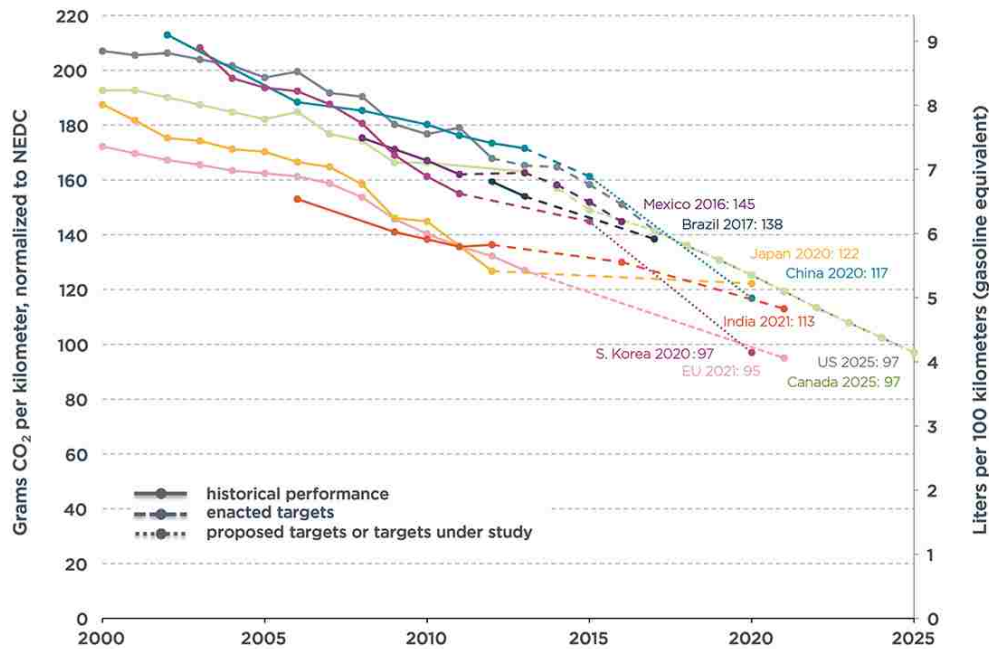


Figure 1.1 CO₂ emissions (g CO₂ /km) normalized to NEDC [1]

By law, new cars registered in the EU must not emit more than 130 grams of CO₂ per kilometer (g/km) by 2015, which corresponds to an equivalent fuel consumption of around 5.6 liters per 100 km (L/100km) of petrol or 4.9 L/100km of diesel [2]. According to Figure 1.1, the average emissions level of a new car sold in 2015 was around 120 g CO₂ /km, satisfying the 2015 requirement. By 2020 the limitation of CO₂ emission will be 95 g/km. Given the limitation of the current technology of internal combustion engines (ICEs), however, achieving a reduction of 35 g CO₂/km before 2021 is a difficult job. Only 30-35% of the energy of the fuel is converted into usable work by a SI engine and 35-40% by a CI engine [33]. Improvement is still possible; however, some alternative methods must be developed to meet the upcoming regulations. For example, electric vehicles (EVs) are regarded as a valuable solution, since they do not generate pollutants locally and can potentially rely on the energy provided by renewable sources [5].

Nevertheless, despite the continuous developments in battery technology, cost, range capability, and long recharging time are still viewed as barriers to the widespread adoption of such vehicles [5]. The Fuel Cell Vehicle (FCV) or Fuel Cell Electric Vehicle (FCEV) is also an available solution. It is an electric vehicle that uses a fuel cell instead of or in combination with a battery or supercapacitor. This supplies its on-board electric motor, generally using oxygen from the air and compressed hydrogen. Most fuel cell vehicles are classified as zero-emission vehicles that emit only water and heat. Japanese manufacturers show a great interest in this technology and the first commercially produced hydrogen fuel cell automobile began to be sold by Toyota in 2015. However, until now, there has been limited hydrogen infrastructure, and there are only 36 hydrogen fueling stations for automobiles publicly available in the US [17]. A Hybrid Electric Vehicle (HEV) is considered a promising solution to the problem.

1.2 HEV introduction

An HEV is a type of vehicle that combines a conventional internal combustion engine (ICE) system with an electric propulsion system (hybrid vehicle drivetrain) [3]. The Electric powertrain provides better fuel economy and fewer emissions than a conventional vehicle [3]. The reason is that hybrid-electric produces less emissions from its ICE than a comparably sized gasoline car, since an HEV's gasoline engine is usually smaller than a comparably sized pure gasoline-burning vehicle (natural gas and propane fuels produce lower emissions), which if not used to directly drive the car, can be geared to run at maximum efficiency, further improving fuel economy [3]. Table 1.1 shows the effect of electrification on CO₂ emission and fuel consumption by an example. The data in Table 1.1 are from the USA clean vehicles website, which presents the general value of CO₂ emission and the equivalent fuel consumption for conventional vehicle, battery electric vehicle, and plug-in hybrid electric vehicle.




Vehicle type	Icon	CO ₂ Emission [g/km]	Equivalent Fuel consumption [l/100km]
Gasoline-only		236.8	8.11
Plug-in Hybrid Electric		129.9	4.52
Battery Electric		95.7	3.31

Table 1.1 CO₂ emissions comparison among different kinds of vehicles [4]

In general, there are two different types of HEVs: series hybrid and parallel hybrid. Two hybridization ratios are respectively used to define the electrification level of both kinds of HEVs. The series hybridization ratio is defined as

$$R_{h,SERIES} = \frac{P_{GEN}}{P_{EM}}$$

where, P_{GEN} is the power of the electric generator and P_{EM} is the power of the electric motor. Alternately, the parallel hybrid is defined as

$$R_{h,PARALLEL} = \frac{P_{ICE}}{P_{ICE} + P_{EM}}$$

where, P_{ICE} is the power of the internal combustion engine and P_{EM} is the power of the electric motor.

Figure 1.2 shows that a pure electric vehicle with batteries has a hybridization ratio of zero for either the parallel or series hybrid vehicle. If the hybridization ratio of parallel HEV reaches one, it indicates an ICE vehicle without any electrification. For a series HEV, if the hybridization ratio is one, it indicates a vehicle with electric transmission, where a battery or a capacitor serves as an energy buffer. The thesis focuses on the range extender series hybrid vehicle.

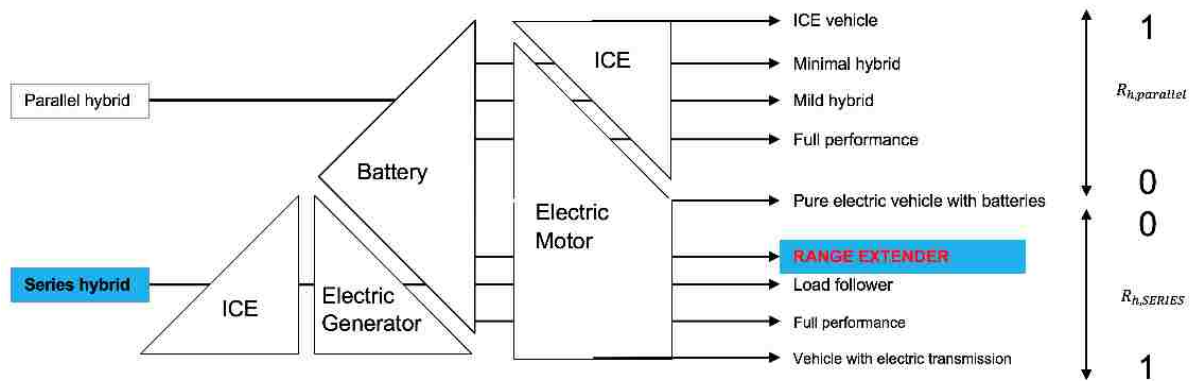


Figure 1.2 HEV classification

1.3 Range extender

A range extender is a type of series HEV for which there is an electrical generator coupled with a relatively small internal combustion engine to recharge the battery. The energy is available from the on-board rechargeable energy storage system (i.e. the battery), and the auxiliary energy supply (i.e. ICE combined with an electrical generator) is only enabled when the energy of the battery is no longer available. The addition of an auxiliary power unit (i.e. ICE) provides the

benefit of extending the range of the vehicle and alleviating the driver's range anxiety. Furthermore, the mechanical disconnection between the ICE and the drivetrain offers some advantages concerning to the cost, packaging and design of the energy management system, since the speed of the engine can be adjusted depending on the power request and engine's efficiency so as to minimize the fuel consumption [5]. In Figure 1.3, the configuration of the vehicle structure is presented, and the power electronic unit linked to the battery pack is the power inverter.

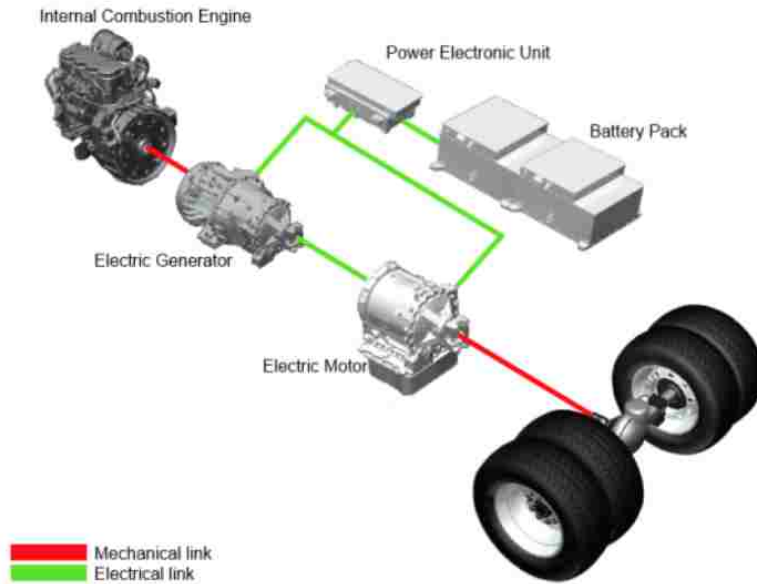


Figure 1.3 Range extender structure [7]

2 LITERATURE REVIEW

Many different aspects of HEVs have been investigated in the past few years. This chapter consists of two parts: modeling approach and control strategy. The modeling approach usually determines the accuracy of the model, and it is necessary to guarantee that the model is suitable for the simulation. The control strategy is the central part of an HEV and it is generally developed to meet some specific requirement, which could be the driveability, vehicle performance or the emission target.

2.1 Modelling methodologies

Three different methods of modelling methodologies are summarized by Millo et al. [11]: kinematic approach, quasi static approach, and dynamic approach.

2.1.1 Kinematic approach

The kinematic approach is based on a backward methodology, where the input variables are the vehicle velocity and the road grade angle (Genta, 1997). Starting from the input driving cycles, the traction force and speed can be calculated from simple kinematic relationships (Figure 2.1 (a)). The engine speed and torque are finally determined from the previous results and the information about the powertrain (Figure 2.1 (b)). Therefore, a 0-D black box model of the engine is used to compute the instantaneous fuel consumption or emission rate, as shown in Figure 2.2. The cumulative data can be obtained over the driving cycle by integrating the instantaneous fuel consumption and emission rate.

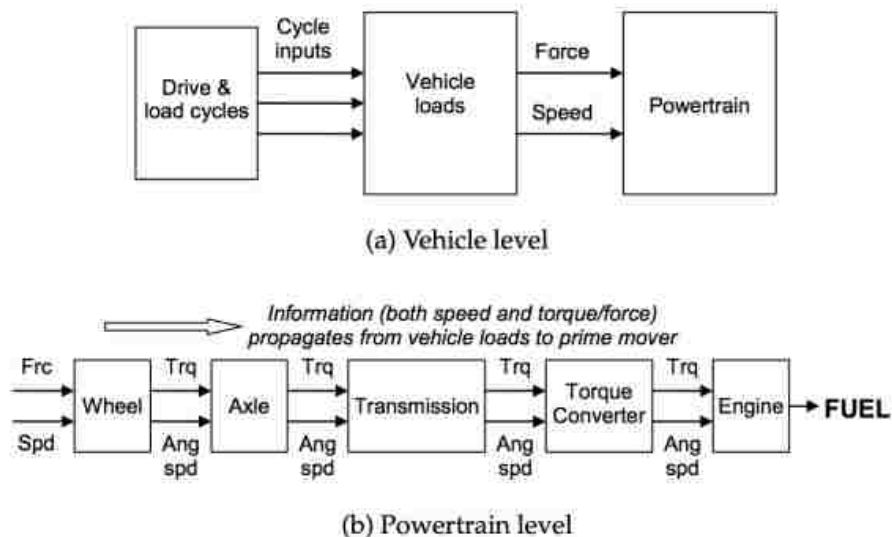


Figure 2.1 Information flow in a kinematic simulator (from Guzzella & Sciarretta 2007)

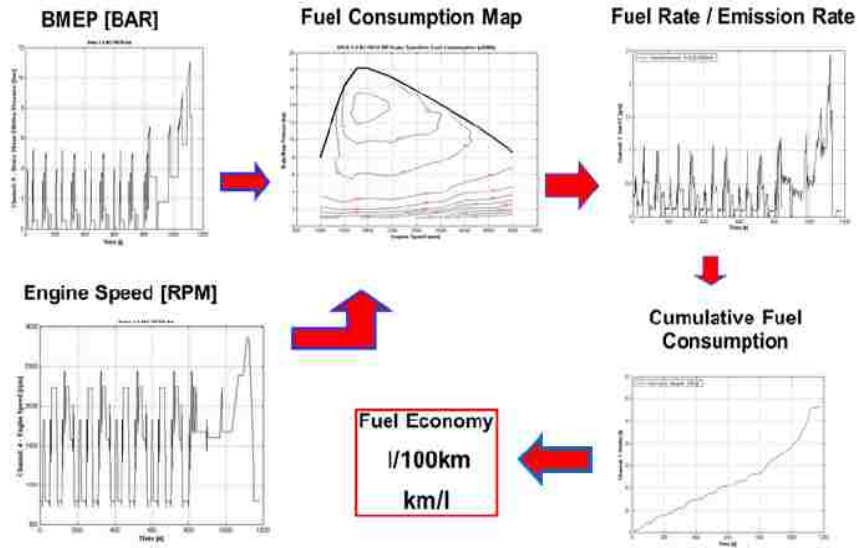


Figure 2.2 Information flow in a backward model for motor vehicles fuel consumption calculation [11]

The shortcoming of this approach is that it cannot be applied during transient conditions, since it neglects all the dynamic phenomena. It is often used for preliminary evaluation of the fuel consumption or engine emissions. However, most of the papers applying dynamic programming as the control strategy take advantage of this method, in terms of the simplicity and computational efficiency of the model.

2.1.2 Quasi static approach

In the quasi static approach, a driver model (typically a PID) compares actual speed with the target vehicle speed and generates a power demand profile to reduce the difference, by solving the longitudinal vehicle dynamics equation as shown in Figure 2.3 (Guzzella & Sciarretta, 2007; GAMMA TECHNOLOGY, 2009). The fuel consumption or pollutant emissions are calculated by interpolating the engine maps with the same method for kinematic approach.

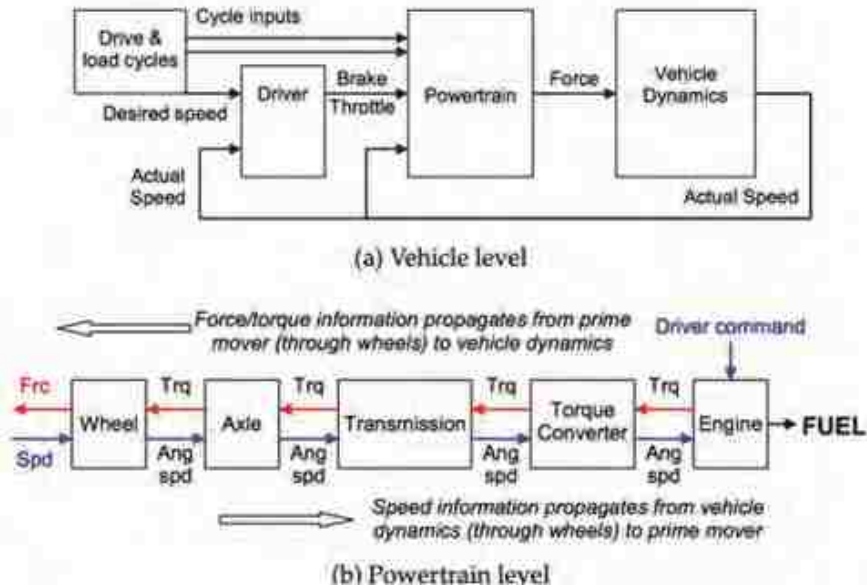


Figure 2.3 Information flow in a quasi-static powertrain model [11]

The simulation model is viewed as a quasi-static model, although the system dynamics are taken into consideration, the behaviour of main devices (ICE, EM, batteries) is still described by means of steady state performance maps. This method can be suitable, considering the simulation targets and the requirements of the powertrain characteristics. The model with this method is more accurate than that of the kinematic approach.

2.1.3 Dynamic approach

In the full dynamic approach, not only the longitudinal vehicle dynamics equation is solved to determine the engine speed and torque, but also the ICE behavior during transient conditions is modelled by means of detailed 0D or 1D fluid-dynamic models. In this case, highly dynamic events, such as abrupt vehicle accelerations during tip-in manoeuvres can be properly simulated with a reasonable accuracy. This method is adopted by Arsie et al. [13] to describe the driver-vehicle interaction for a generic transient and to simulate the vehicle driveline, the ICE and the electric motor/generator, aiming at optimization of the control strategy with provisional load estimate.

2.2 Control strategies

In the high supervisory Power Management Layer (PML), many algorithms have been developed. Depending on powertrain architecture, five types of control strategies are explained by Flah et al.,

which are offline power management control (PMC) strategies, online PMC strategies, rule-based PMC strategies, learning PMC strategies and GPS-enhanced PMC strategies [14].

2.2.1 Offline Power Management Control Strategies

Dynamic programming has been generalized as the main methodology to solve sequential decision-making problems. It has two principal features: an underlying discrete time dynamic system whose state evolves according to given transition probabilities that depend on the decision taken at each time and a cost function that is additive over time. Although DP can yield a global optimal solution, for many problems, a complete solution by DP is impossible [14]. DP is widely used for the investigation of HEV control strategies problems. For example, Hung et al. applied this method to derive the optimal power-splitting factor for the hybrid system for preselected driving schedules, with an established model of truck class two series hydraulic hybrid [15]. Lin et al. also used DP techniques to determine the optimal control actions for a hybrid powertrain in order to minimize fuel consumption of a parallel hybrid electric truck over a given drive cycle [18]. In addition, Ao et al. investigated the fuel economy improvement and NO_x emission reduction and demonstrated the trade-off between fuel economy and the emission of nitrogen oxides for a state of charge sustaining parallel HEV by applying dynamic-programming-based supervisory controller (DPSC) [20].

2.2.2 Online Power Management Control Strategies

Model predictive control (MPC) relies on prediction models to obtain a control action by solving an online optimization problem over a finite horizon. It is often applied in constrained regulatory related control problems of large scale multivariable systems, where the objective is to operate the system in a certain desired way. Arise et al adopts this method for developing the control strategy for a parallel hybrid vehicle. An estimate of future vehicle load is performed with a neural network to optimize the supervisory control strategy during the estimated future time window [13].

Another online PMC strategy is equivalent control management strategy (ECMS). One of its principal procedures in solving optimization problems is to derive a set of necessary conditions that must be satisfied by any optimal solution. These conditions become sufficient under certain convexity conditions on the objective and constraint functions. Optimal control problems may be regarded as optimization problems in infinite-dimensional spaces, and thus, they are substantially

difficult to solve. Zentner et al proposes a framework for causal optimal control of diesel engines with this method [21].

2.2.3 Rule-based Power Management Control Strategies

Rules Based (RB) method relies on expert experience base to determine fine adjustments to be applied in PMC strategy. The PMC strategy can be based on fuzzy logic, decentralized adaptive logic, or even new set of rule based PMC strategies. Sorrentino et al. assessed the performance of a RB control strategy for series hybrid vehicles via comparison with a batch Genetic Algorithm-based optimization [22]. In his paper, a hybrid solar vehicle (HSV) was considered, requiring to define the heuristic rules as function of both average traction power and current solar irradiation. The RB control architecture consists of two tasks, external and internal. As for the external task, it needs to define the desired final state of charge (SOC) to be reached at the end of the driving cycle to enable full storage of solar energy captured during the following parking phase. In terms of the internal task, it is required to estimate the average power delivered by ICE electric generator and SOC deviation from final SOC as function of average traction power. In addition, Hung et al. obtained implementable rules by extracting the optimal trajectory features from a DP scheme for the development of an optimal control strategy of a truck class two series hydraulic hybrid vehicle [15].

2.2.4 Smart/ Learning Power Management Control Strategies [14]

To optimize efficiency, PMC strategies include a learning mechanism that allows improving performance over time, every single reaction of the driver is considered including driving style, sprint, breaking style, and distances driven. All this collected information builds a database specific to the user driving style and there are PM adjustments connected to driving parameters. This has a major impact on fuel economy and system responsiveness [23].

2.2.5 GPS enhanced Power Management Control Strategies [14]

These strategies are to improve PMC strategies using information received from a Global Positioning System (GPS). The strategy uses data and loads corresponding topography of the road and operates according to preconfigured driving style to minimize fuel consumption. These enhancement strategies are using driving pattern recognition to automatically select a control

strategy from a bank of six optimized representative driving modes using artificial neural networks (ANNs).

Apart from different types of control strategies, the goal of optimization and some physical limitations are also taken into consideration while analyzing HEV problems. A weighted cost function consisting of fuel economy and emissions is proposed by Ao et al. to investigate the interaction effect of emission control and the minimization of fuel economy [20]. In the thesis work of Moura, the interplay of battery sizing and optimal power management was mentioned [24]. The object is to quantify the extent to which different PHEV power management algorithms enable the use of smaller batteries without compromising performance and efficiency. Because literature shows that operating PHEVs in a full electric battery depletion mode often requires batteries with both high energy and power characteristics, thus resulting in more expensive components [25-28]. With blending control strategies, it utilizes engine power throughout the depletion process to ration battery energy and reduce electric power requirements by shifting load to the combustion engine. Xia et al. presented an innovative design concept and method to obtain a power management strategy for HEVs, which is independent of future driving conditions. A quadratic performance index is designed to ensure the vehicle drivability, maintain the battery energy sustainability and average and smooth the engine power and motor power to indirectly reduce fuel consumption [29]. Mill et al. considers the constraints of additional noise, vibration and harshness (NVH) caused by ICE operations for the design of an optimal strategy for a range-extended electric vehicle, since it influences the comfort of the passengers [5].

3 CASE STUDY

This thesis topic is put forward by Fiat Research Center (CRF) powertrain group. The main purpose is to design the control strategy for a range-extended plug-in hybrid electric vehicle (PHEV) by means of dynamic programming optimization. The vehicle used for simulation is a B-segment hatch-back passenger car. Table 3.1 presents the data of the vehicle.





Vehicle Model (PHEV)		
	Prototype	B-SEGMENT CAR
Electric Motor& Generator		
	Max Power	75 kW
	Max Torque	330 Nm
	Max Speed	7000 RPM
Battery Characteristic		
	Energy	18 kWh
	Cell Number	121
	Capacity	40 Ah
Engine Data		
	Max Power	55 kW @ 6000 RPM
	Max Torque	110 Nm @ 3250 RPM
	Displacement	1.4 L
	Type of fuel	Gasoline

Table 3.1 Vehicle data

The simulations are performed in two different operating modes—charge depleting and charge sustaining—along seven driving cycles: New European Driving Cycle (NEDC), Worldwide Harmonized Light Duty Test Cycles (WLTC), Federal Test Procedure (FTP75), Highway Fuel Economy Driving Schedule (HWFET), the New York City Cycle (NYCC), United States Supplemental Federal Test Procedure (US06), and Supplemental Federal Test Procedure (SC03). The figures for all the driving cycles are provided in the Appendix.

Clarification of Road Load Coefficients

Road load (RL) is the force imparted on a vehicle while driving at constant speed over a smooth level surface from sources such as tire rolling resistance, driveline losses, and aerodynamic drag [30]. Road load coefficients are generally obtained by applying the coastdown method. Table 3.2 shows the RL coefficients for WLTC and NEDC provided by Fiat Chrysler Automobiles (FCA). The RL coefficients for WLTC lead to higher power demand than that for NEDC. According to European regulation, the simulations along the NEDC cycle are carried out using the RL coefficient for NEDC, defined in regulation 83 [34]. For WLTC and US cycles, simulations are carried out using the RL coefficients for WLTC.

Road Load Coefficient for WLTC (TMH)			mass
F0 [N]	F1 [N(km/h)]	F2 [(N/(km/h) ²)]	1551.5 kg
153.4	0.277	0.0367	

Road Load Coefficient for WLTC (TML)			mass
F0 [N]	F1 [N(km/h)]	F2 [(N/(km/h) ²)]	1484.5 kg
106.9	0.277	0.0343	

Road Load Coefficient for NEDC			mass
F0 [N]	F1 [N(km/h)]	F2 [(N/(km/h) ²)]	1432.5 kg
96.5	0.269	0.0333	

Table 3.2 RL coefficients for WLTC and NEDC

3.1 Vehicle Modeling

The range extended PHEV model adopts the kinematic approach, that is introduced in the previous chapter. In addition, to realize the model in a MATLAB environment for simulations, electric machines, the internal combustion engine (ICE) and the battery are modelled using steady state maps measured by experiment and available from the FCA and Politecnico di Torino

database. Although this methodology neglects transient phenomena, it has been proven to be suitable when used for this work [11].

3.1.1 Electric Machine Model

Figure 3.1 shows the mechanical characteristic and efficiency map of the electric machines. To be specific, an electric machine could be either an electric motor or a generator. The vehicle model includes both an electric motor and a generator, and they have the same values of maximum power, torque and speed, as illustrated in Table 3.2. The generator works during regenerative braking or when the battery is charged by the ICE.

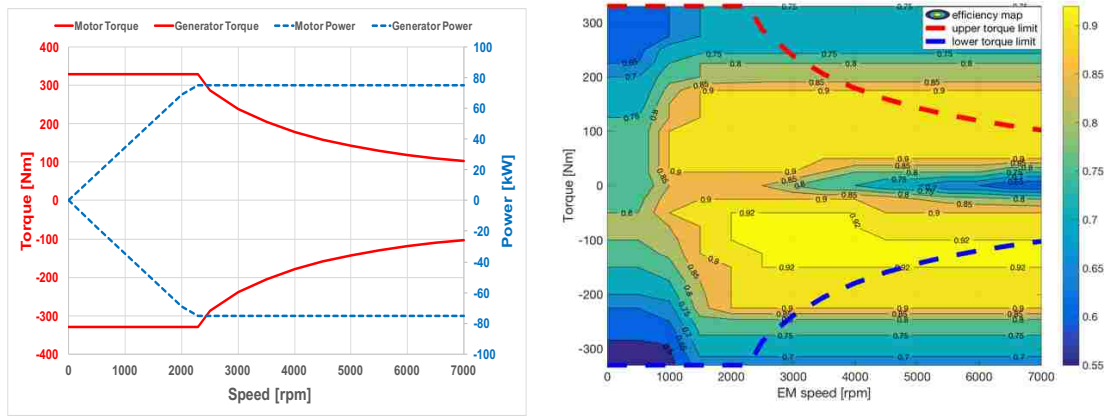


Figure 3.1 Mechanical characteristic and efficiency map of the electric machines

Relevant formulae are presented here:

$$P_{res} = (F_0 + F_1 * v + F_2 * v^2) * \frac{v}{3.6} \dots\dots (3.1)$$

$$P_{em} = P_{traction} / \eta_{gearbox} \dots\dots (3.2)$$

$$P_{inertia} = \delta * m * a * \frac{v}{3.6} \dots\dots (3.3)$$

$$T_{em} = \frac{P_{em}}{2\pi N} \dots\dots (3.4)$$

$$P_{traction} = P_{res} + P_{inertia} \dots\dots (3.5)$$

Mechanical and magnetic losses account for the reasons why the area of high EM speed and low torque shows relatively low efficiency on the efficiency map in Figure 3.1. Mechanical losses are caused by the movement of the motor. These include the friction in the motor bearings, and drag on the rotor caused by turbulence of the air around it (windage loss) [39]. Mechanical losses are considerably high, when the motor rotates at high speed. If the load applied on the rotating part also goes down, the effect of friction force will be aggravated and it leads to higher mechanical

losses. Together, this leads to lower efficiency. In addition, magnetic loss is crucial in a high-speed permanent magnet motor. These losses are associated with magnetic paths of the motor. Magnetic losses include hysteresis losses, caused by the changing polarity of the flux in the core, and eddy currents, which are induced in the steel core by the changes in flux polarity [38, 39].

3.1.2 Internal Combustion Engine Model

The choice of the ICE for the simulation is the FIRE 1.4 L engine developed by FIAT and previously installed in the FIAT PUNTO. The engine efficiency map is shown in Figure 3.2. Thanks to the mechanical disconnect between the ICE and the drivetrain, the ICE is available to work with its maximum efficiency area: 2000-3000 rpm, 7-9 bar bmep.

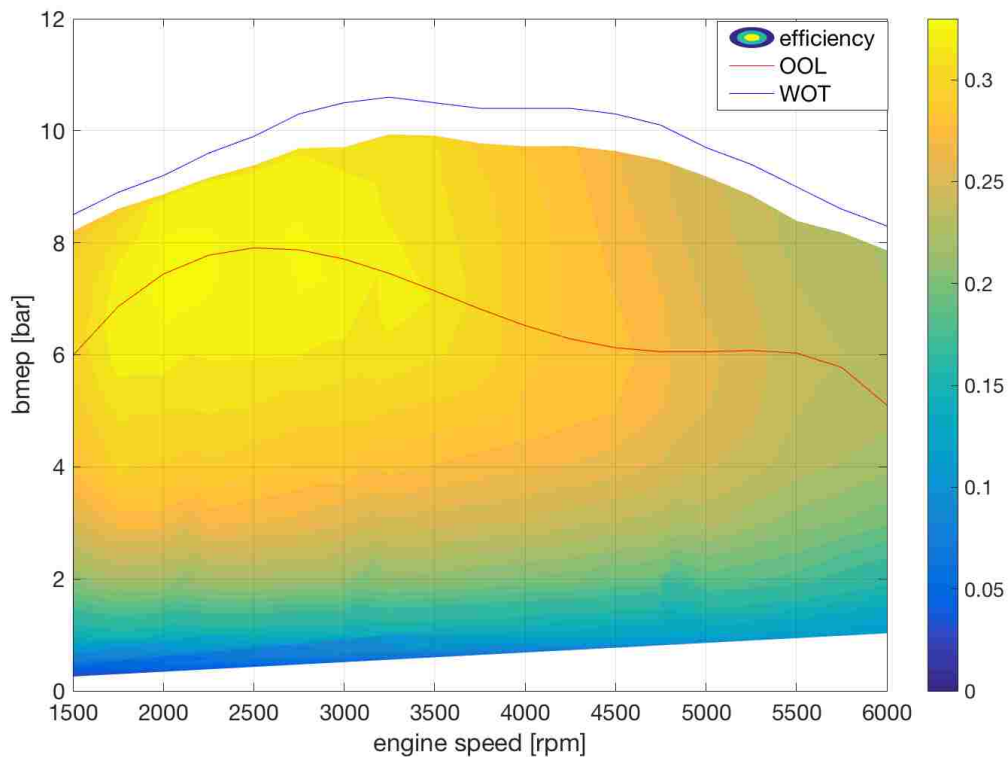


Figure 3.2 Engine efficiency map with optimal operating line (OOL) and wide open throttle (WOT) line

3.1.3 Battery Model

The R_{int} equivalent circuit model shown in Figure 3.3 was used for modeling stationary battery behavior for predictive control because of its fast simulation time. The R_{int} equivalent circuit model contains a constant voltage source in series with a resistor. The battery current can be

computed, according to Ohm's law. The open circuit voltage (OCV) and internal resistance (R_0) are function of battery SOC, neglecting the effect of temperature [31].

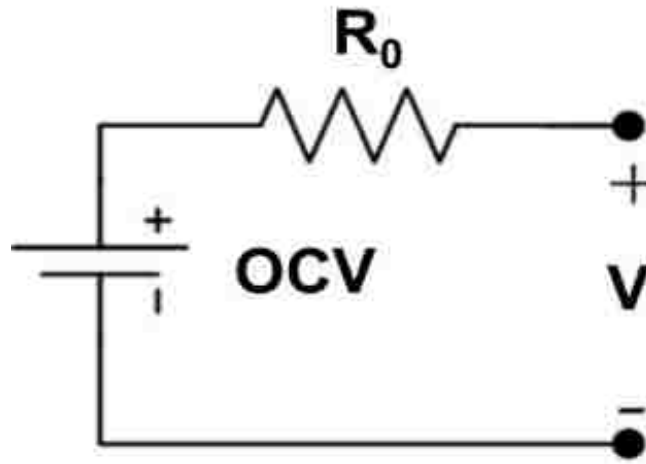


Figure 3.3 R_{int} equivalent circuit model [31]

The relationship among terminal voltage (V), current (I) and the battery power is presented

$$I = \frac{(OCV - V)}{R_0}$$

$$P_{battery} = n * V * I$$

In the literature, other equivalent circuits model the effects of polarization in the battery using RC parallel circuits. Although these models may be more accurate than the R_{int} model, the differential equations that represent capacitors require more simulation time [31]. This cost outweighs the benefits for the purpose for this work, so the R_{int} equivalent circuit is selected.

3.1.4 Braking system

A regenerative brake is an energy recovery mechanism that slows a vehicle or object by converting its kinetic energy into a form that can be used immediately or stored until needed [32]. The amount of power recovered can be assumed as 60% of the traction power during the regenerative braking event, since the electric machines are only mounted on the front axle. In this case, the kinetic energy is transformed to electrical energy through electric generator and is then stored in the battery. For the rear axle, the braking force is provided by the mechanical braking

device and the excess kinetic energy is converted to unwanted and wasted heat by friction in the brakes. The power recovered by the battery during the event is equal to

$$P_{battery} = 0.6 \cdot \eta_{electric\ generator} \cdot \eta_{gear\ box} \cdot P_{traction} \dots \dots (3.6)$$

3.2 Operating modes

There are in general two different operating modes for the R-EX. One is the charge depleting mode (EV mode). In this mode of vehicle operation, the auxiliary power unit (APU) is turned off whenever the battery SOC is above the minimum level. After the battery SOC has reached to the minimum level, the vehicle will arrive at the destination operating the powertrain in the so-called charge sustaining mode, in which the internal combustion engine provides the energy required to keep the battery in charge sustaining conditions [9].

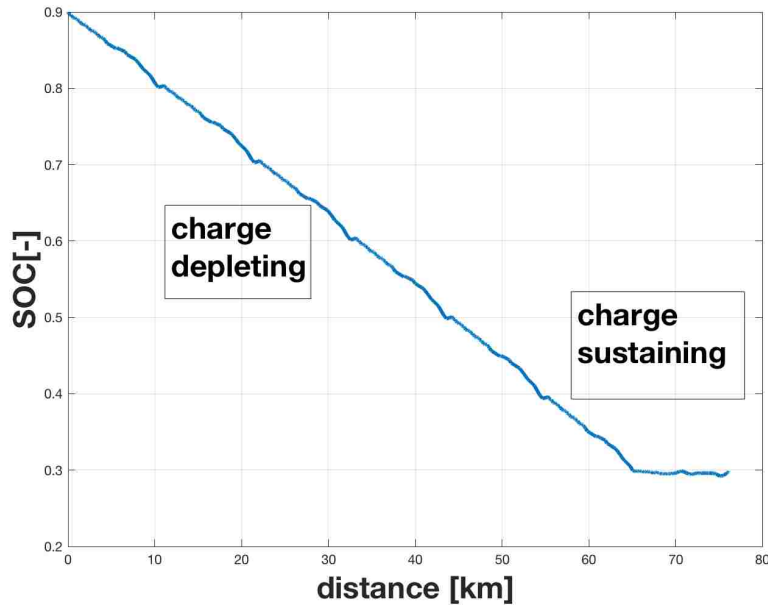


Figure 3.4 Charge depleting and charge sustaining modes

3.3 Methodology

The minimization of CO₂ emission is the main target to achieve, whether the vehicle runs in EV or SERIES mode over different driving cycles.

While the vehicle is running in charge depleting condition, it does not emit carbon dioxide locally, since the auxiliary power unit (the ICE) is kept off; however, the consumed electricity could be generated from the burned fuel in the power plant, where it produces carbon dioxide. Therefore,

the carbon intensity of electricity (CIE) is introduced to calculate the CO₂ emission related to electricity production. In addition, the performance of the range-extended hybrid vehicle is analyzed, in terms of electric range, energy consumption.

While the vehicle is running in charge sustaining condition, the CO₂ emission is mainly due to the consumption of gasoline in the internal combustion engine. In this situation, the CO₂ emission due to consumed electricity is negligible, because the battery can be viewed as an energy buffer and the amount of the power extracted from the battery is relatively small. In this case, a dynamic programming (DP) function is implemented to determine the optimal control strategy to realize the minimum CO₂ emission. From the DP results, the minimum values of CO₂ emission over the designated driving cycles are derived, as well as the optimal ICE operating points, the on and off state of the ICE for each time instant.

Afterwards, rules extraction is applied to the DP results to define a set of thresholds, which can be used in the rule-based control strategy.

3.3.1 Dynamic programming (DP)

Dynamic programming is a function that solves discrete time optimal-control problems using Bellman's principle. This principle states: 'an optimal policy or a set of decisions has the property that, whatever the initial state and optimal first decision may be, the remaining decisions constitute an optimal policy with regard to the state resulting from the first decision [35, 36]. It can be expressed as

$$p_{1,N}^* = \{u_1^*, u_2^*, \dots, u_N^*\}$$

where $u_1^*, u_2^*, \dots, u_N^*$ are the decisions or control variables and $p_{1,N}^*$ is a multi-stage optimal policy for the discrete-time deterministic dynamic optimization problem which minimizes the weighed cost J given by

$$J = \sum_{i=1}^N L(x_i, u_i)$$

$$x_{i+1} = f(x_i, u_i)$$

subjected to

$$x_i \in X_i \subset \mathfrak{R}^n, u_i \in U_i \subset \mathfrak{R}^m$$

where x_i and u_i are vectors of state variables and control variables separately. X_i and U_i are compact sets of admissible controls. L is the instantaneous cost function [19, 20, 37].

For the range-extended PHEV, a state variable is the battery state of charge (SOC). The cost function of CO₂ emission can be presented as

$$J = \frac{\mu_{CO_2}}{\mu_{fuel}} \int_0^T \dot{m}_f(t, u(t)) dt + CIE \cdot \Delta SOC \cdot E_{batt}$$

- where μ_{CO_2} and μ_{fuel} are the molar mass of CO₂ and fuel respectively
- \dot{m}_f is the instantaneous fuel consumption of the engine
- $u(t)$ is the vector of the control variable
- T is the duration of the vehicle mission
- Carbon intensity of the electricity (CIE) is the average CO₂ emission related to the production of the electrical energy that is supplied by the grid to recharge the battery
- ΔSOC is the variation of the state of charge
- E_{batt} is the total electrical energy that can be stored in the battery after recharging from the grid

ΔSOC is negligible if the vehicle is in charge sustaining condition, since the variation of SOC is almost zero over the complete driving cycle. The constraints that should be imposed are

$$SOC_{min} \leq SOC(i) \leq SOC_{max}$$

where SOC_{min} and SOC_{max} are set to 0.28 and 0.32 respectively.

DP is capable of determining the optimal solution to this discrete problem; however, the need for a backward procedure means that the solution can be obtained only offline, for a driving cycle known a priori, and therefore it is not possible to use DP for an online implementable solution. Furthermore, the high computational load makes any DP optimization prohibitive on typical on-board microcontrollers [37]. Figure 3.5 presents the application of dynamic programming.

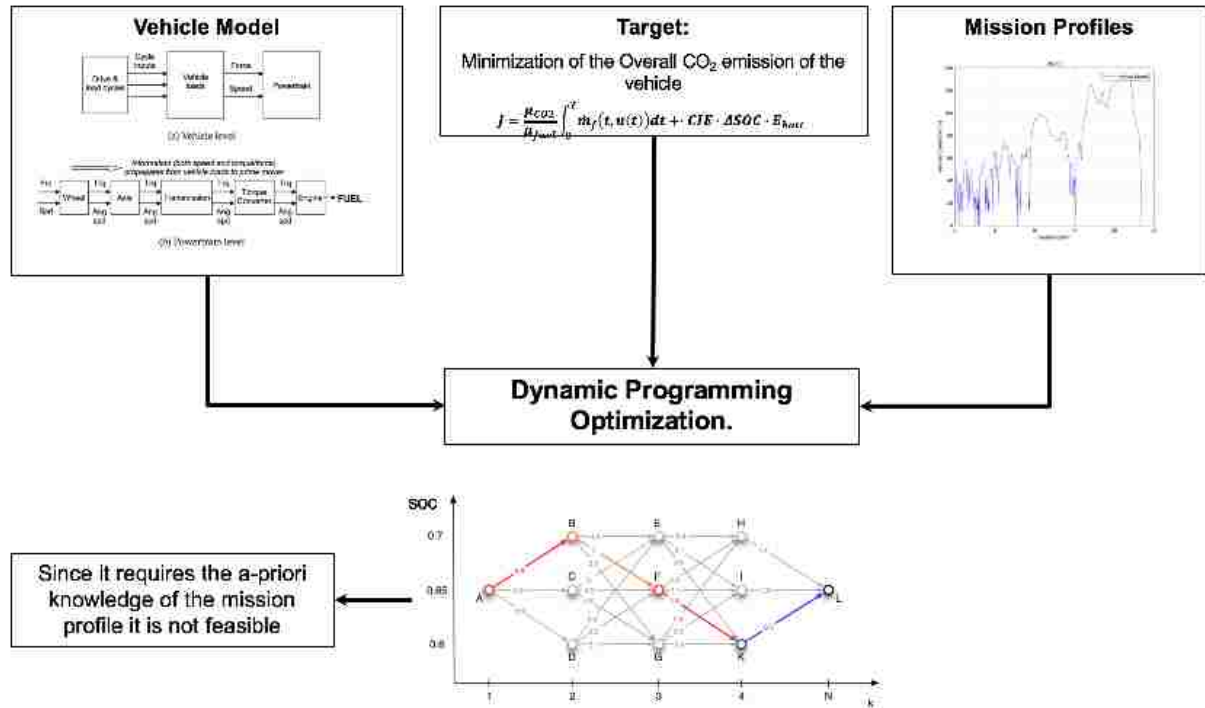


Figure 3.5 Dynamic programming optimization

3.3.2 Rule-based control strategy

As mentioned before, although the dynamic programming approach provides an optimal solution for minimizing carbon dioxide emission, the resulting control policy is not implementable in real driving conditions because the optimal policy requires knowledge of the future speed and load profile of the vehicle. Nonetheless, analyzing optimal policies determined through dynamic programming can provide insight into how the CO₂ emission reduction is achieved. A rule-based control algorithm is proposed based on the investigation of the DP results.

Rule-based control strategy is a method of implementing supervisory control in an HEV by introducing a set of rules that decide the power split between the engine and the energy storage device, given the observed values of some meaningful parameters.

Rules extraction is a feasible way to determine the set of rules to be used for the rule-based control strategy. With all the operating points over 7 driving cycles derived from the DP results, it is carried out by identifying suitable thresholds (SOC, power, vehicle speed, acceleration and so

on), which can be implemented in the vehicle control unit. The information of the selected parameters is likely to be measured or is simple to be calculated.

An example of flow chart of rule structure is presented in Figure 3.6. The rules are usually in the form if-then-else, which is a path that it checks each threshold one by one and afterward makes the final decision.

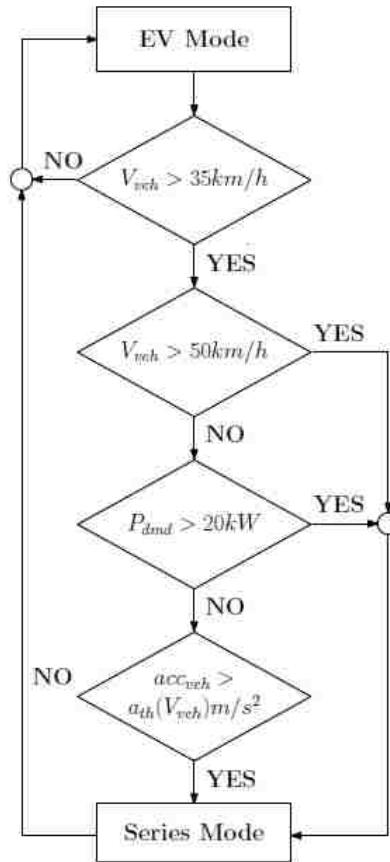


Figure 3.6 Example of rule-based control strategy [7]

4 RESULTS

4.1 Simulation results (charge depleting condition)

For the following results, zero watt represents the hypothetical reference value of the auxiliary power, which could supply navigation, air conditioning, headlights, and so on.

The simulation results for WLTC and NEDC in the charge depleting condition are presented for contrastive analysis. Figure 4.1 presents the variation of vehicle speed over the driving cycles during the simulation. In Figure 4.2, the operating points are plotted in the EM efficiency maps. It can be seen in Figure 4.1 that more accelerations appear in WLTC than those in NEDC, which correspond to higher loads for the electric machines when the vehicle runs along the WLTC in Figure 4.2.

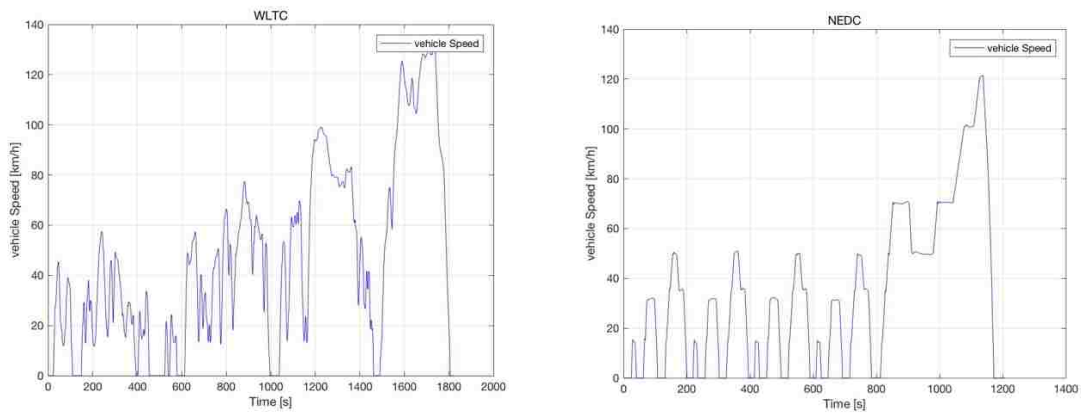


Figure 4.1 Driving cycles for WLTC (left) and NEDC (right)

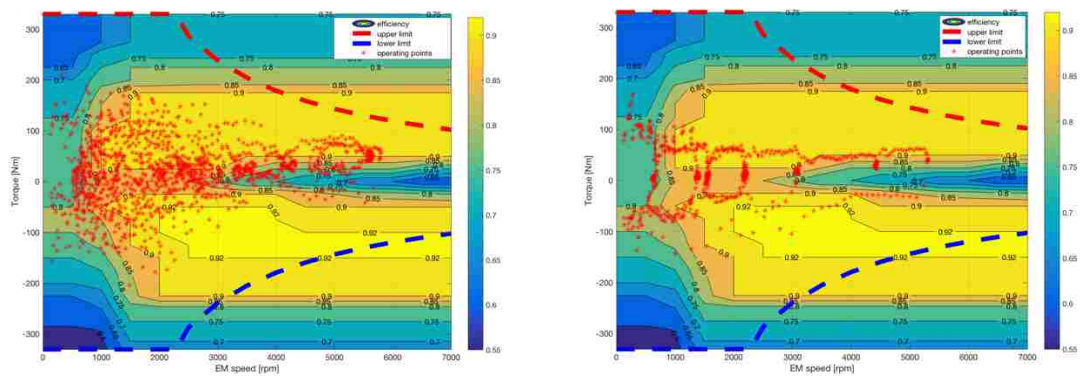


Figure 4.2 Operating points in the EM efficiency map for WLTC (left) and NEDC (right)

Figure 4.3 presents the variation of SOC for both WLTC and NEDC. The initial SOC is 0.9 and it goes down to 0.25 at 70 km and 0.26 at 100 km respectively for WLTC and NEDC, which shows that the vehicle is in charge depleting mode. For nearly the same amount of the energy consumption, the vehicle can reach a further distance along NEDC. To conclude, for a certain vehicle architecture, a relatively demanding road condition leads to high load for electric machines, therefore the energy consumption increases and the electric range decreases.

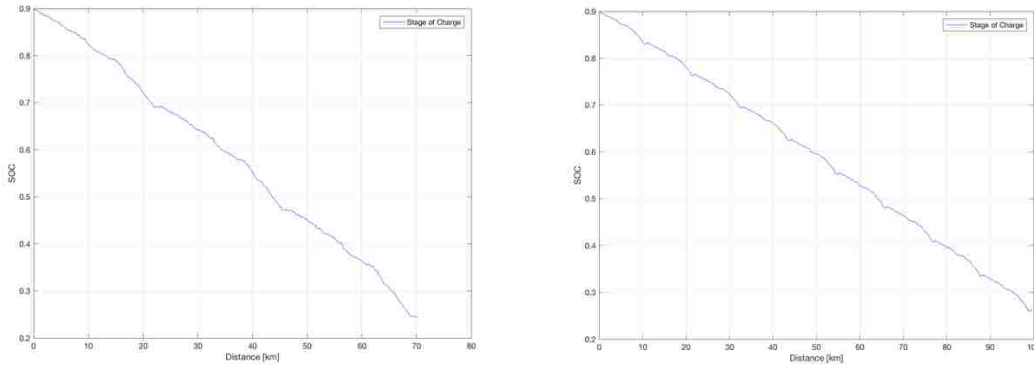


Figure 4.3 Variation of battery SOC for WLTC (left) and NEDC (right)

In Tables 4.1, 4.2 and 4.3, the “max number of cycles” indicates the maximum number of a complete driving cycle the vehicle can cover using 70% of the energy stored in the battery. “SOC_END” indicates the final value of SOC at the end of simulation. “E_consumed” is the total energy consumed during the simulation. “EC” is the energy consumption per one hundred kilometers. “ELECTRIC RANGE” is the distance that the vehicle can cover just relying on the energy stored in the battery. Test mass high (TMH) and test mass low (TML) are two different situations with different road load values. Table 4.1 shows the simulation results for NEDC and WLTC, while Table 4.2 shows the simulation results for all the US driving cycles.

	NEDC	WLTC (TML)	WLTC (TMH)
max # of cycles	9	3	3
SOC_END	0.26	0.33	0.25
E_consumed [kWh]	11.5	10.3	11.7
EC [kWh/100km]	11.5	14.6	16.6
ELECTRIC RANGE [km]	99.6	70.3	70.3

Table 4.1 Simulation results of NEDC and WLTC (TMH and TML)

	SC03	US06	HIGHWAY	FTP75	NYCC
max # of cycles	15	4	5	5	36
SOC_END	0.22	0.24	0.22	0.22	0.22
E-consumed [kWh]	12.2	11.6	12.2	12.1	12.2
EC [kWh/100km]	14.1	22.6	14.8	13.7	17.9
ELECTRIC RANGE [km]	86.4	51.6	82.5	88.8	68.3

Table 4.2 Simulation results of all the US driving cycles

To conclude, the most and least demanding driving cycles are US06 and NEDC respectively with regard to the amount of energy consumption, which are 23 kWh/100 km and 12 kWh/ 100 km respectively. Correspondingly, the electric ranges for US06 and NEDC are the shortest and longest, which are 52 km and 100 km. An electric range of 100 km is not an optimistic outcome by comparison with the conventional vehicle range. This also accounts for the reason why the R-EX is developed as a promising method to address the driver’s range anxiety problem.

4.1.1 Sensitivity analysis

Sensitivity analysis is the study of how the uncertainty in the output of a mathematical model or system (numerical or otherwise) can be apportioned to different sources of uncertainty in its inputs [8]. In this section, the effects of two inputs on the carbon dioxide emission are evaluated: the auxiliary power and the carbon intensity of electricity (CIE).

4.1.1.1 Auxiliary Power

In recent years, the fuel efficiency or carbon dioxide emission of modern HEV powertrains has progressed to a point where low voltage auxiliary electrical system loads have a pronounced impact on fuel economy and CO₂ emission. While improving the energy consumption of an individual component may result in minor improvements, the collective optimization of such loads across a complete vehicle system can result in meaningful gains [12]. Therefore, a sensitivity analysis about the effect of the overall auxiliary power on CO₂ emission is performed.

The results of three typical test cycles (NEDC, FTP75, WLTC) for road conditions in Europe, in the US and around the world have been recalculated by considering the auxiliary power ranging from 0 to 2000 W with a step of 500 W.

Table 4.3 concludes the simulation results of electric range and energy consumption, which are plotted in Figure 4.4. The distances of a complete driving cycle of NEDC, FTP75, and WLTC are 11.1 km, 17.7 km, and 23.4 km respectively. The drop of 23.4 km at 1000 W on WLTC in Table 4.3 is because of an increment of 500 W auxiliary power. The battery can supply the traction power for the vehicle to accomplish three complete WLTCs with 500 W auxiliary power. But if there is a rise of 500 W auxiliary power, the battery can only provide the energy for two complete WLTCs with 1000 W auxiliary power. The same reason explains why the electric range remains the same on FTP75 from 500 W to 1500 W. The energy in the battery is sufficient for the vehicle to finish four complete FTP 75 cycles, while it is still enough with an extra auxiliary power of 500 W, 1000 W or 1500 W. Figure 4.4 shows that the energy consumption is proportional to the increment of the auxiliary power.

ELECTRIC RANGE [km]				ENERGY CONSUMPTION [Wh/km]			
	NEDC	FTP75	WLTC		NEDC	FTP75	WLTC
0 W	99.6	88.8	70.3	0 W	115	136	166
500 W	88.5	71.1	70.3	500 W	130.2	151.2	176.5
1000 W	77.4	71.1	46.9	1000 W	145.3	165.9	187.3
1500 W	77.4	71.1	46.9	1500 W	160.5	181	198
2000 W	66.4	53.3	46.9	2000 W	175.6	195.2	208.9

Table 4.3 Electric range and energy consumption with the variation of auxiliary power

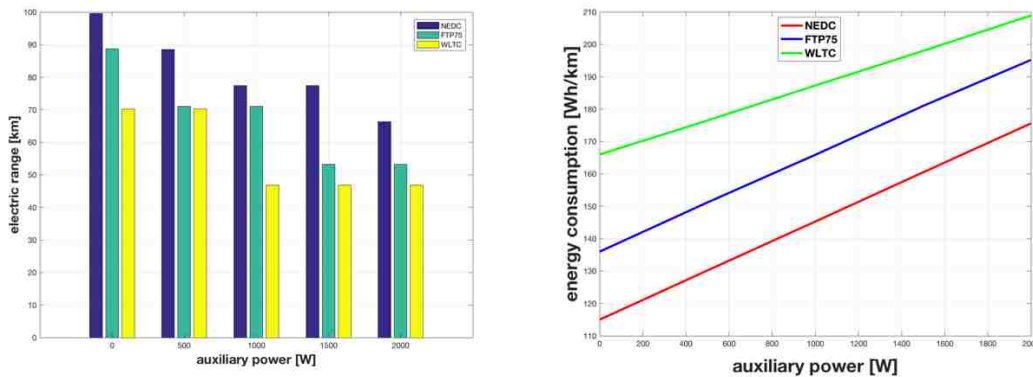


Figure 4.4 Electric range (left) and energy consumption (right) with the variation of auxiliary power

4.1.1.2 Carbon Intensity of Electricity

CO₂ emission from fossil combustion in electricity production contributes significantly to total greenhouse gas emissions. Therefore, it is meaningful to compute the equivalent CO₂ emission of the consumed electrical energy for vehicles in the charge depleting condition. Carbon Intensity of Electricity (CIE) is an available factor for calculating carbon dioxide emissions from electricity consumption. It varies from 71 g/ kWh like France which relies heavily on nuclear energy to 1333 g/ kWh for some developing countries which primarily burns coal as shown in Table 4.4.

Different areas	CIE (g/kWh)
France	71
Europe	423
United States	547
China	973
India	1333

Table 4.4 CIE values for different areas in the year of 2011 [16]

For the sensitivity analysis of the auxiliary power, the driving cycles of NEDC, FTP75, and WLTC (TMH) were chosen to analyze the effect of CIE on CO₂ emission.

Simulation results in Table 4.5 show that the solution of R-EX may not reduce the automobile CO₂ emission in an effective way for developing countries, since the CO₂ emission due to the production of electricity is relatively high. From the literature, HEVs do not promise much benefit in reducing CO₂ emissions in some developing countries currently, but greater CO₂ reduction could be expected in future if coal combustion technologies improve and the share of non-fossil electricity increases significantly [18].

	CO ₂ Emission (g/km)		
	NEDC	FTP75	WLTC (TMH)
France (71 g/kWh)	8	10	12
Europe (423 g/kWh)	48	58	70
United States (547 g/kWh)	62	75	91
China (973 g/kWh)	111	133	162
India (1333 g/kWh)	152	182	222

Table 4.5 Results of CIE sensitivity analysis

4.1.2 Performance Verification

Two parameters are evaluated to check the performance of the vehicle, one is the acceleration time t from 0 to 100 km/h, the other one is the maximum slope α that the vehicle can overcome. The value of these two parameters only relates to RL coefficients. They are calculated according to the following equations:

$$\frac{1}{a} = \frac{\delta * m}{\frac{T_{wheel} * i_g}{R_{wheel}} - F_{res}} \dots \dots (4.1)$$

$$t = \int_{v_1=0 \text{ km/h}}^{v_2=100 \text{ km/h}} \frac{1}{a} dv \dots \dots (4.2)$$

$$\tan(\alpha) = \frac{\frac{P_{em} * \eta_{gearbox}}{v} - F_{res}}{m * g} \dots \dots (4.3)$$

Empirically, the acceleration time ranges from 7 to 10 s for a passenger car, and the performance of two typical range-extended HEVs–BMW i3 and Chevrolet Volt–can be taken as reference. The acceleration time of the BMW i3 and Chevrolet Volt are 7.9s and 7.5s respectively from the vehicle specification data on their official websites. Generally, the minimum requirement of the grade ability in percentage for passenger cars is around 30%. Table 4.6 presents that the acceleration time can be achieved is around 10 s. and the maximum slope that can be overcome is over 30% for all the conditions.

	RL NEDC	RL WLTC TML	RL WLTC TMH
Acceleration time[s]	9.58	9.95	10.53
Maximum slope [deg]	20.41 (37.21%)	19.72(35.84%)	18.77 (33.98%)

Table 4.6 Acceleration time and maximum slope

4.2 Simulation Results (Charge Sustaining Condition)

In this section, dynamic programming results for the vehicle in charge sustaining condition are presented: the output power, engine optimal operating points, states of engine, variation of SOC, and minimum CO₂ emission over driving cycles. The simulation results of WLTC are explained and the results of all the other driving cycles are presented below.

4.2.1 WLTC

The time length and distance of WLTC are 1823 seconds and 23.4 kilometers. Figure 4.5 shows the simulation results in terms of the output power. The upper two plots present that the trajectory of the demand power resembles that of the EM power. The difference between them is because of the power losses considering the drivetrain transmission efficiency. The left lower plot shows the output of ICE power over the driving cycle. There are two main ICE operating points; one point is of 16.5 kW, with BMEP 7.5 bar and ICE rotational speed 2000 rpm, the other point is of 24 kW, with BMEP 8 bar and rotation speed 2600 rpm. Figure 4.6 shows that the two points are located on the optimal operating line of the engine map and their point numbers are 774 and 50 respectively, while there are 1824 points of time in total for WLTC.

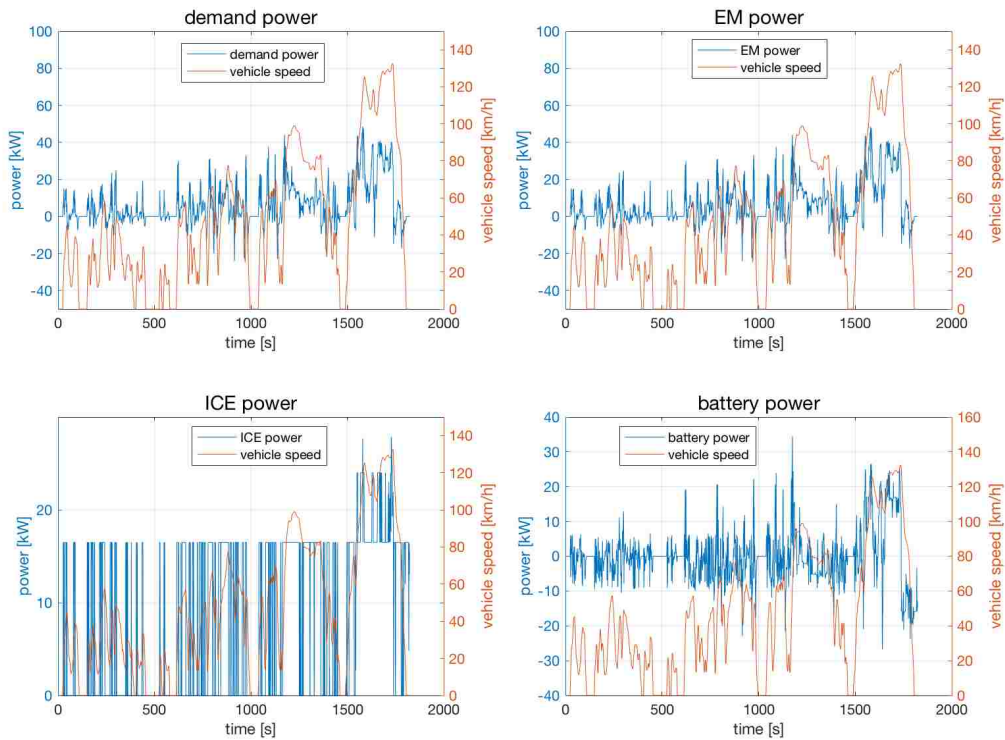


Figure 4.5 Results for demand power, EM power, ICE power, and battery power for WLTC

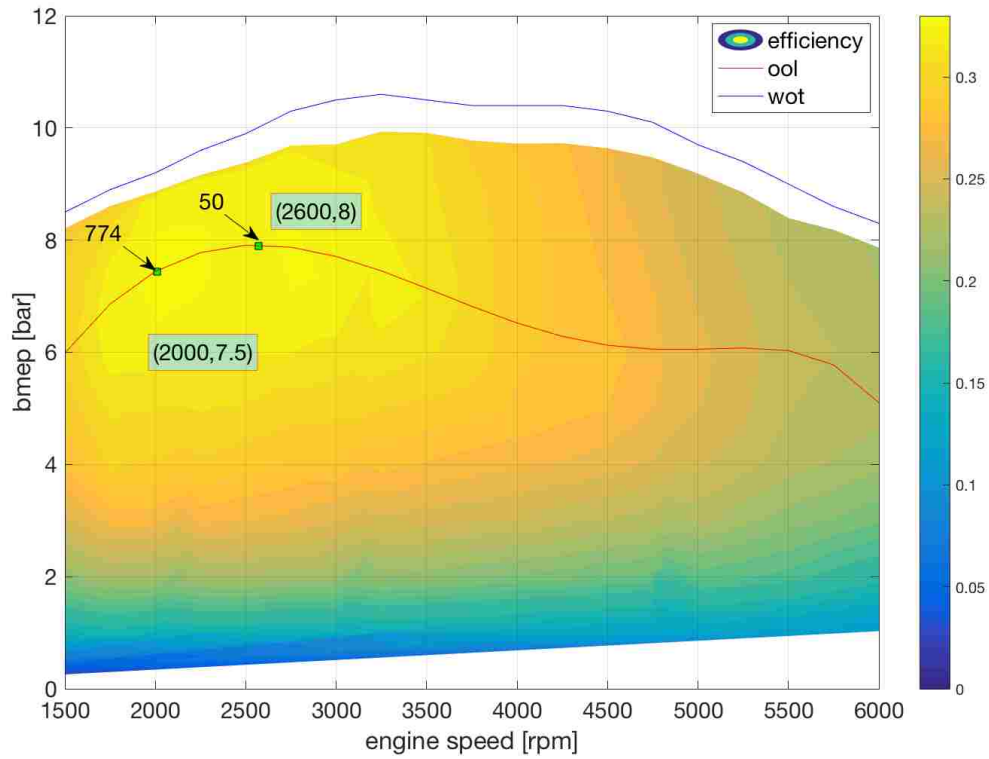


Figure 4.6 Optimal operating line and full load line for WLTC

Figures 4.7 and 4.8 show the switch of the vehicle operating modes over the WLTC. If the color of a point or line is blue in both figures, it indicates that the ICE engine is off; the vehicle is in EV mode at that time instant. While if the color is red, it indicates that the ICE engine is on, the vehicle is in SERIES mode. In Figure 4.8, it can be noticed more clearly that the engine is, in general, turned on, when the vehicle starts to accelerate, and it is shut down for the deceleration.

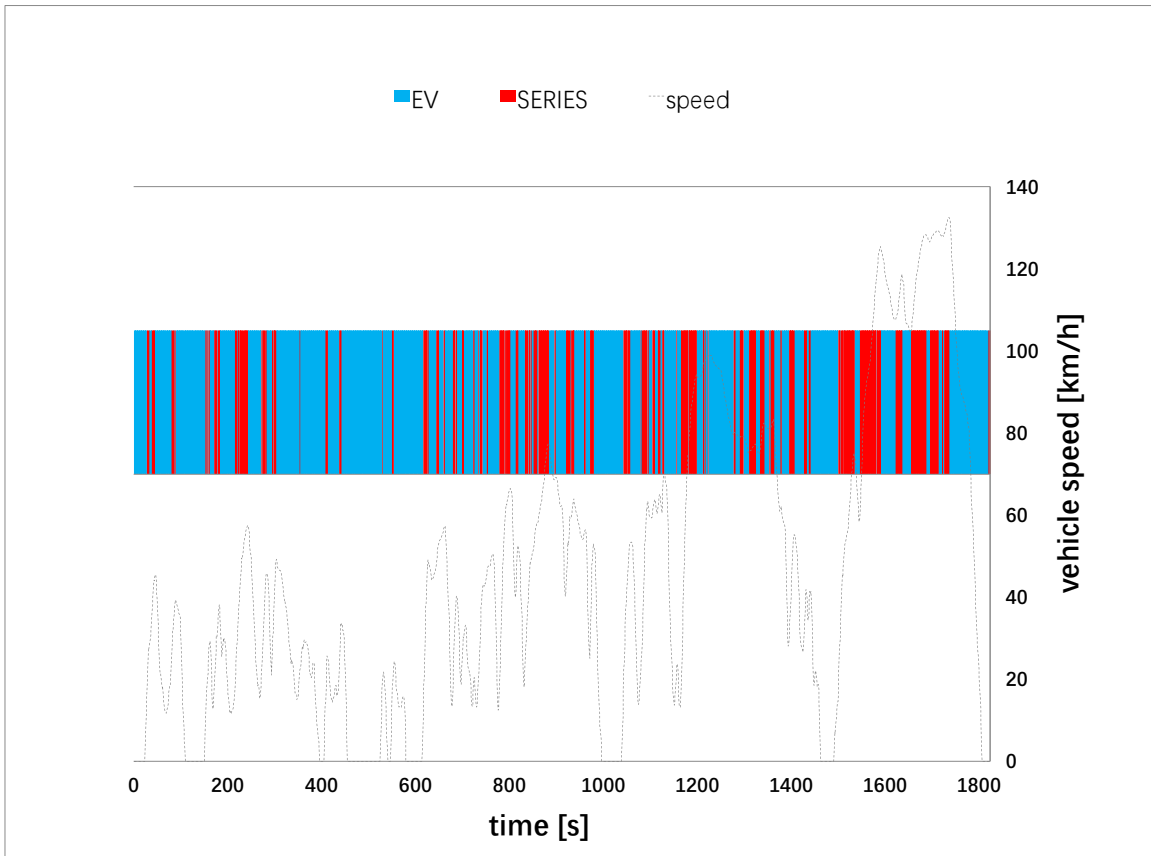


Figure 4.7 Vehicle operating modes switching over WLTC

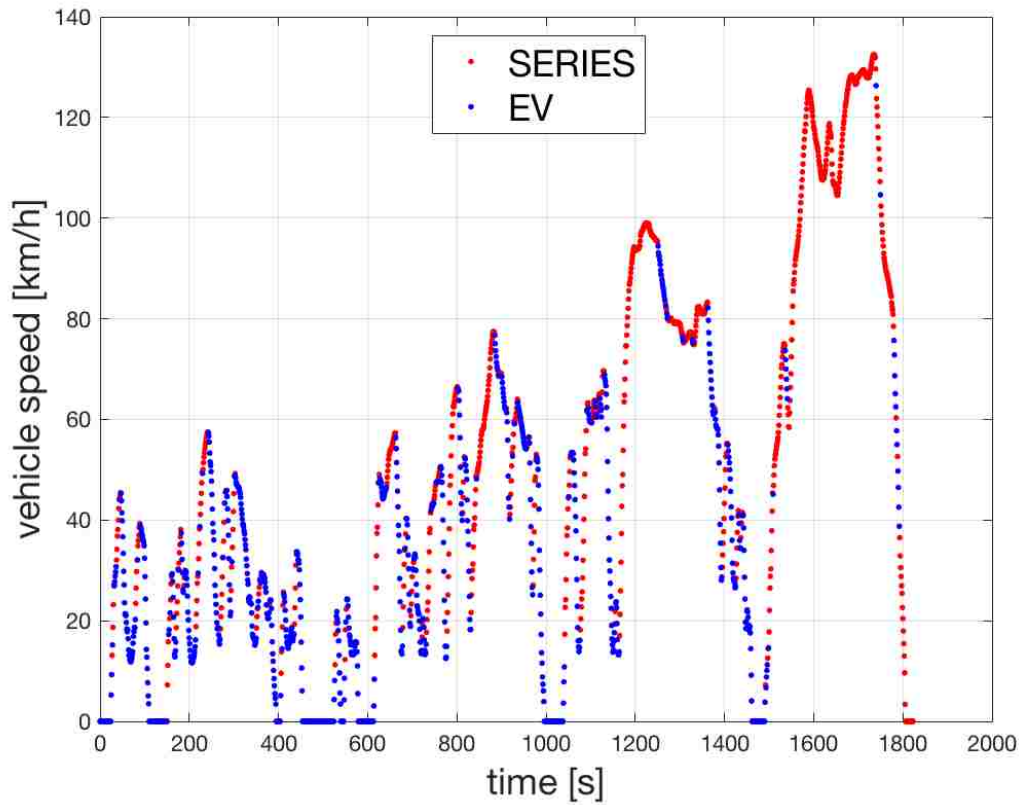


Figure 4.8 Vehicle operating modes switching over WLTC (point by point)

4.2.2 NEDC

The time length and distance of NEDC are 1205 seconds and 11.06 kilometers.

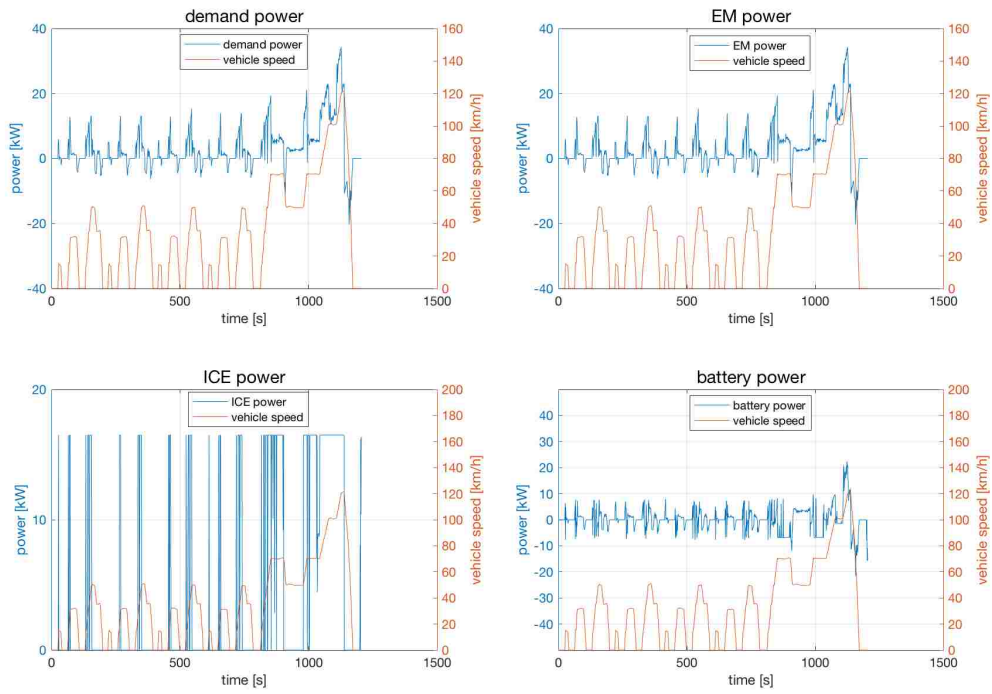


Figure 4.9 Results for demand power, EM power, ICE power, and battery power for NEDC

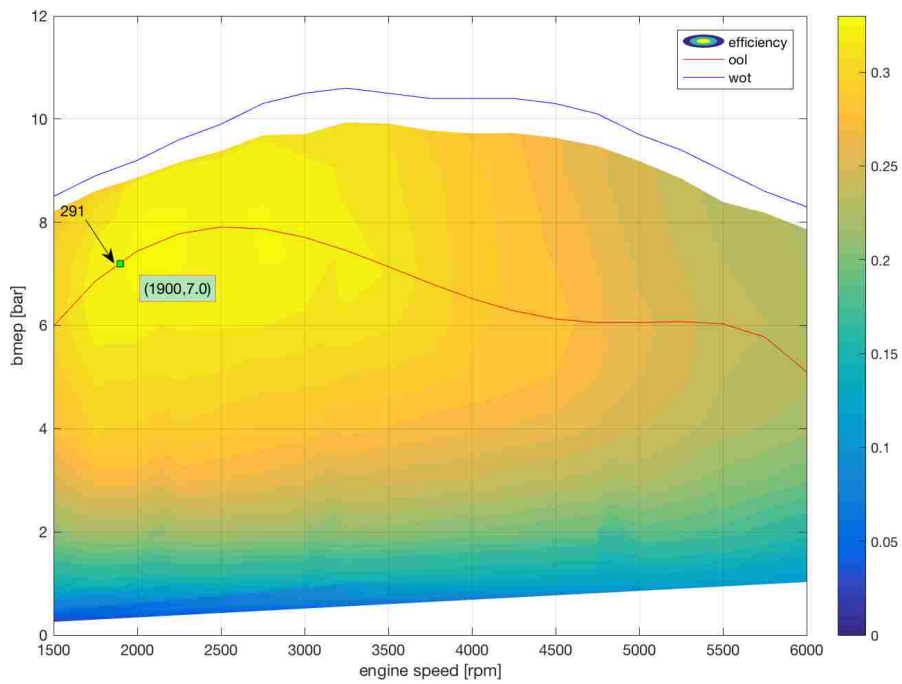


Figure 4.10 Optimal operating line and full load line for NEDC

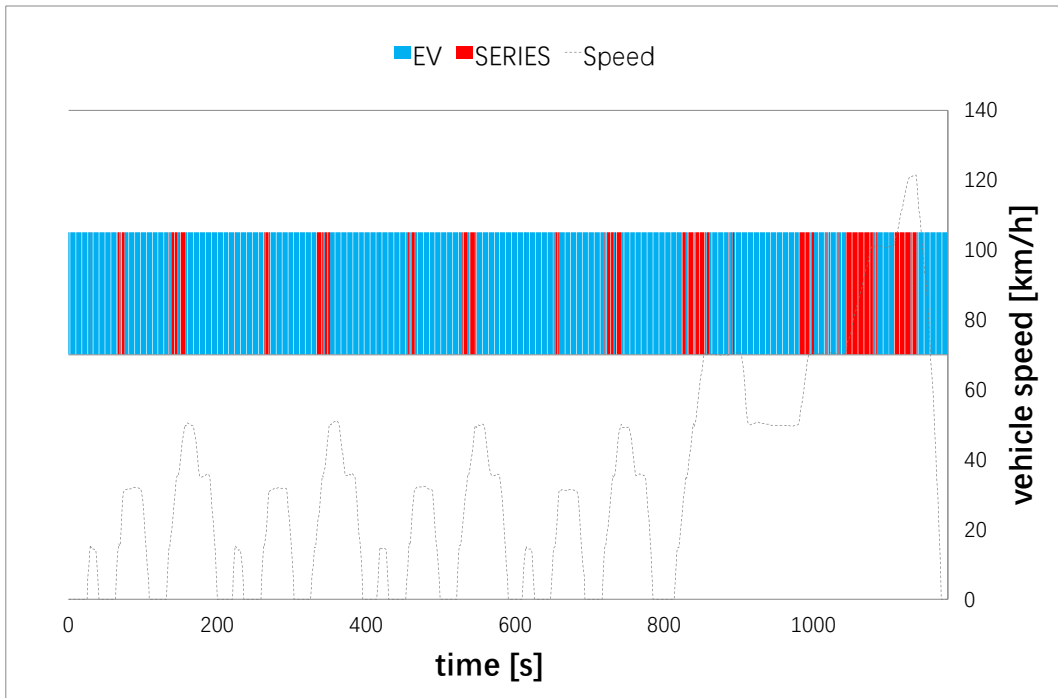


Figure 4.11 Vehicle operating modes switching over NEDC

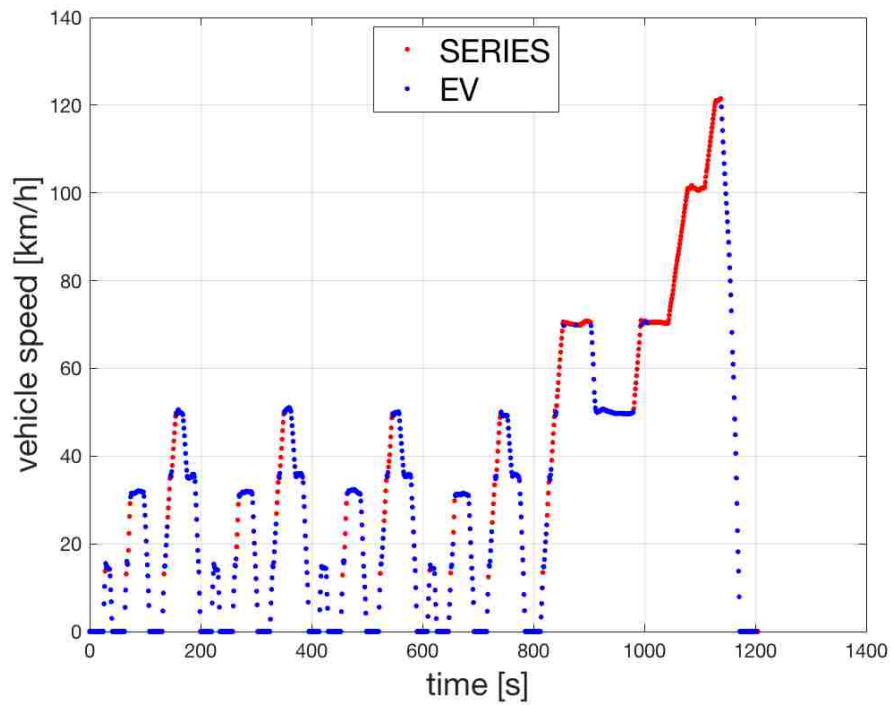


Figure 4.12 Vehicle operating modes switching over NEDC (point by point)

4.2.3 US06

The time length and distance of US06 are 600 seconds and 12.89 kilometers.

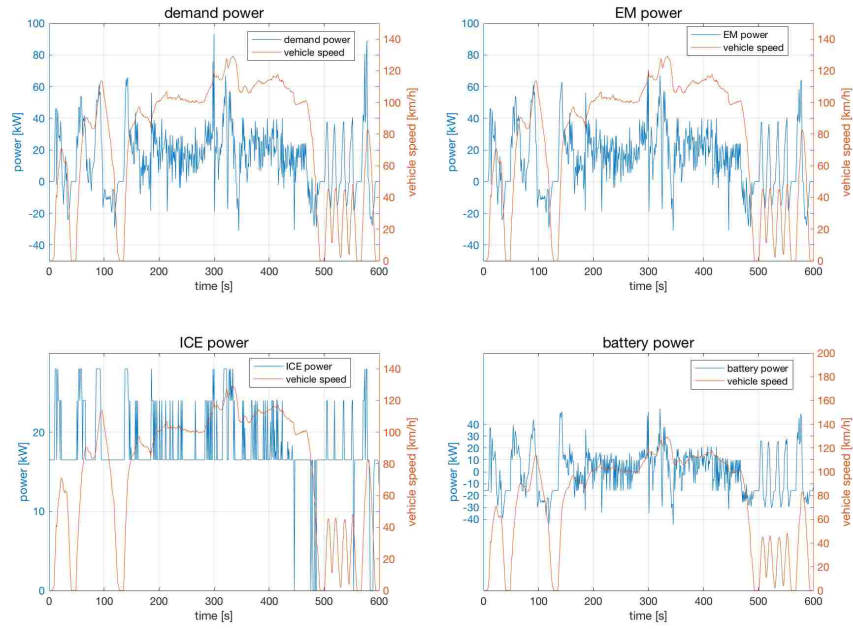


Figure 4.13 Results for demand power, EM power, ICE power, and battery power for US06

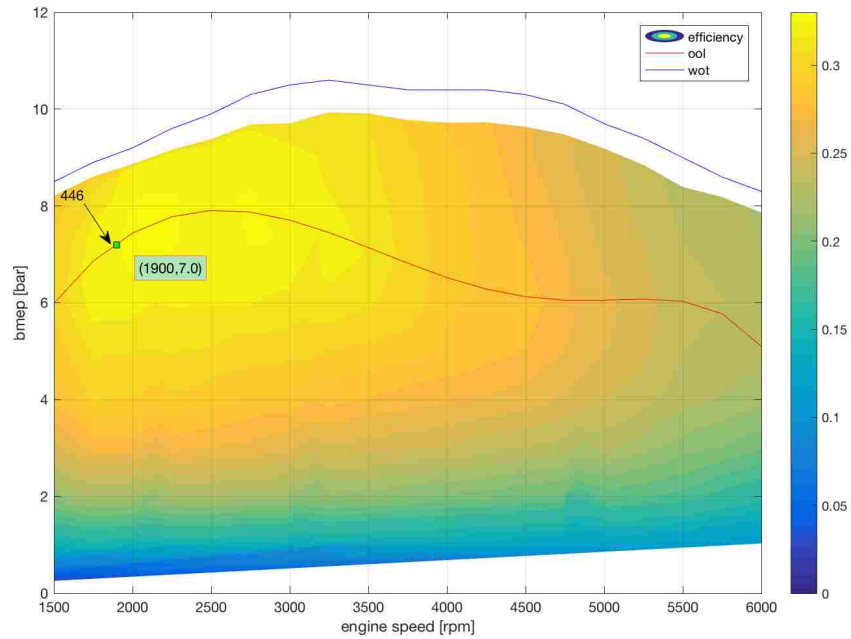


Figure 4.14 Optimal operating line and full load line for US06 cycle

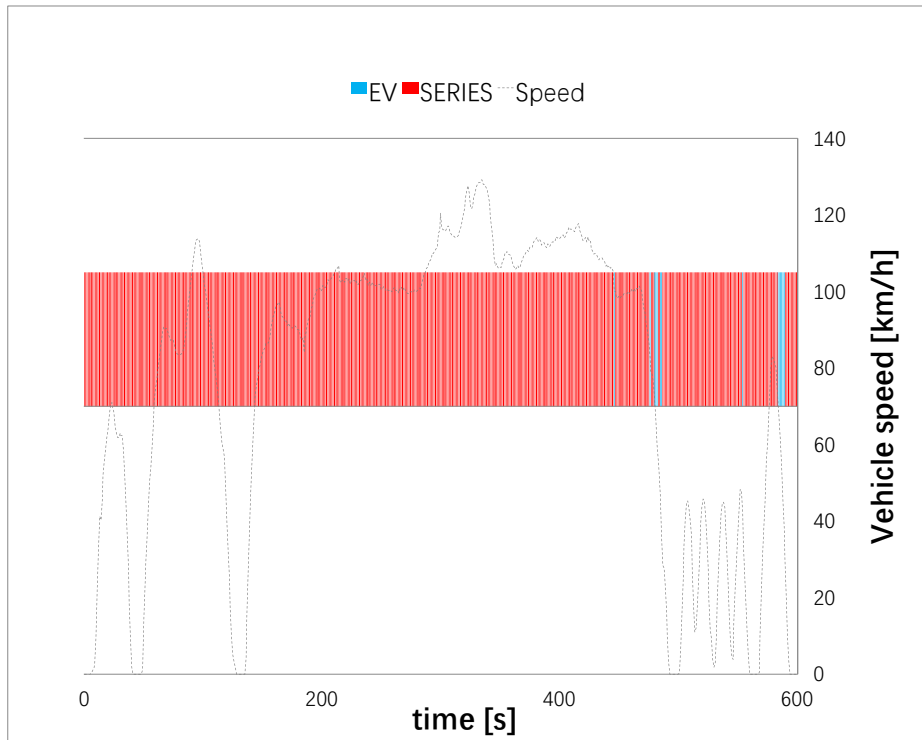


Figure 4.15 Vehicle operating modes switching over US06 cycle

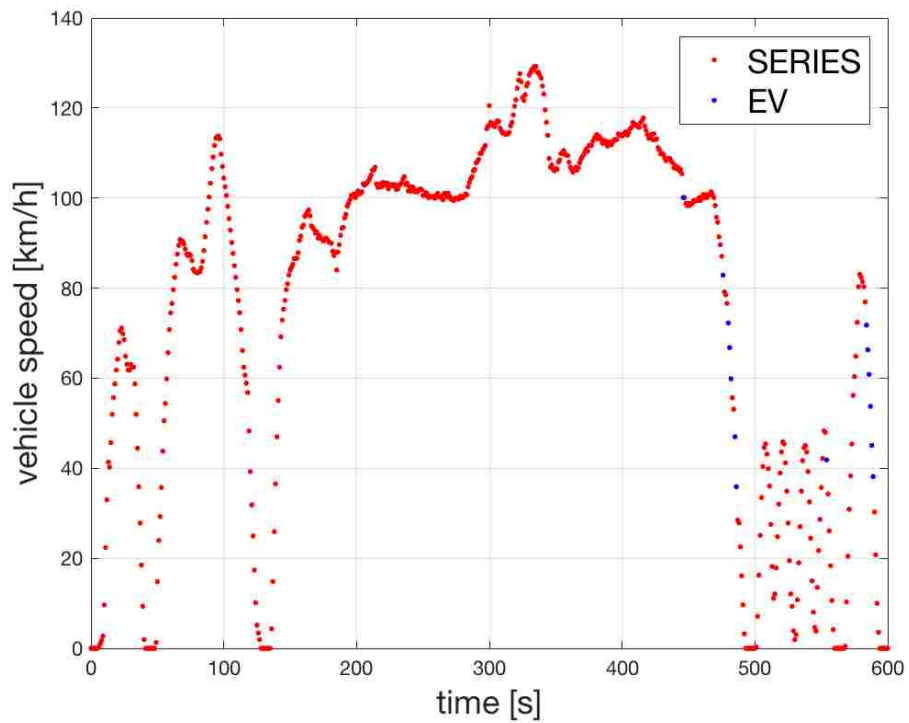


Figure 4.16 Vehicle operating modes switching over US06 cycle (point by point)

4.2.4 SC03

The time length and distance of SC03 are 600 seconds and 11.06 kilometers.

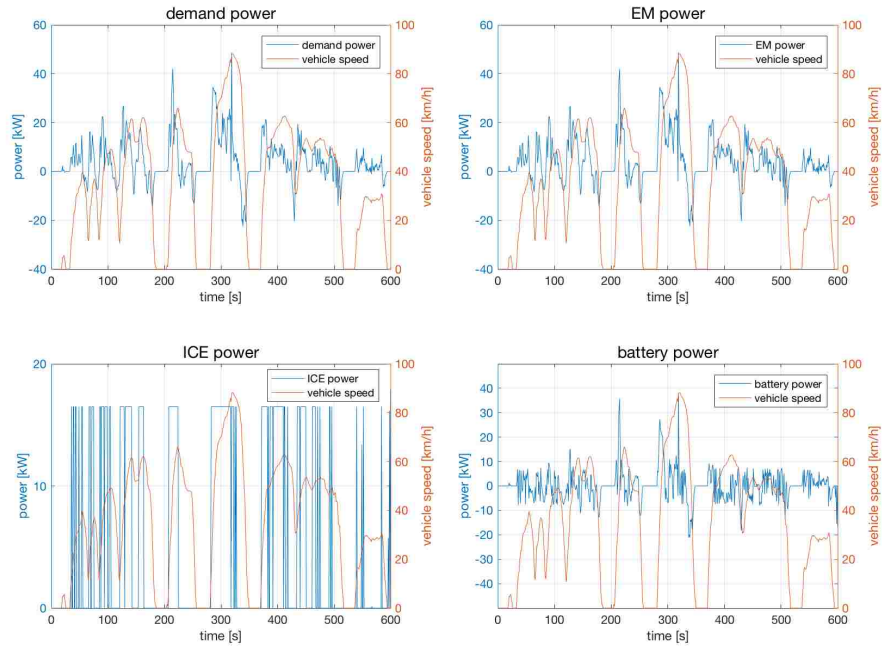


Figure 4.17 Results for demand power, EM power, ICE power, and battery power for SC03 cycle

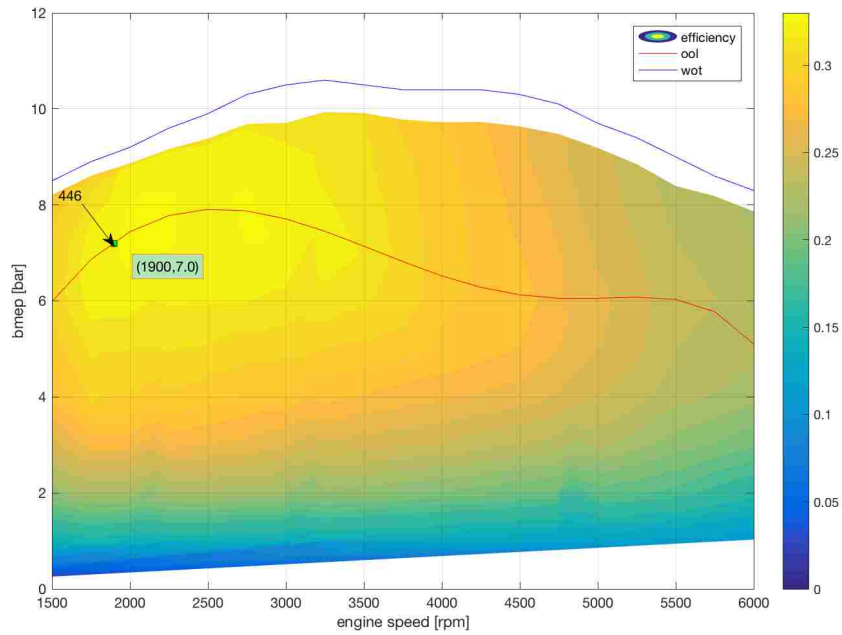


Figure 4.18 Optimal operating line and full load line for SC03 cycle

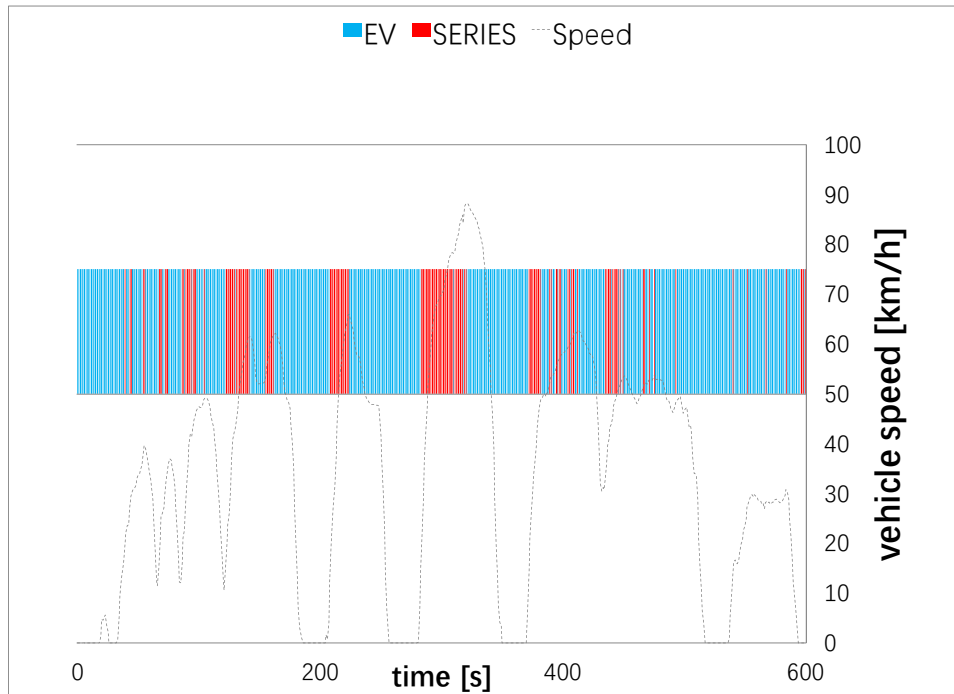


Figure 4.19 Vehicle operating modes switching over SC03 cycle

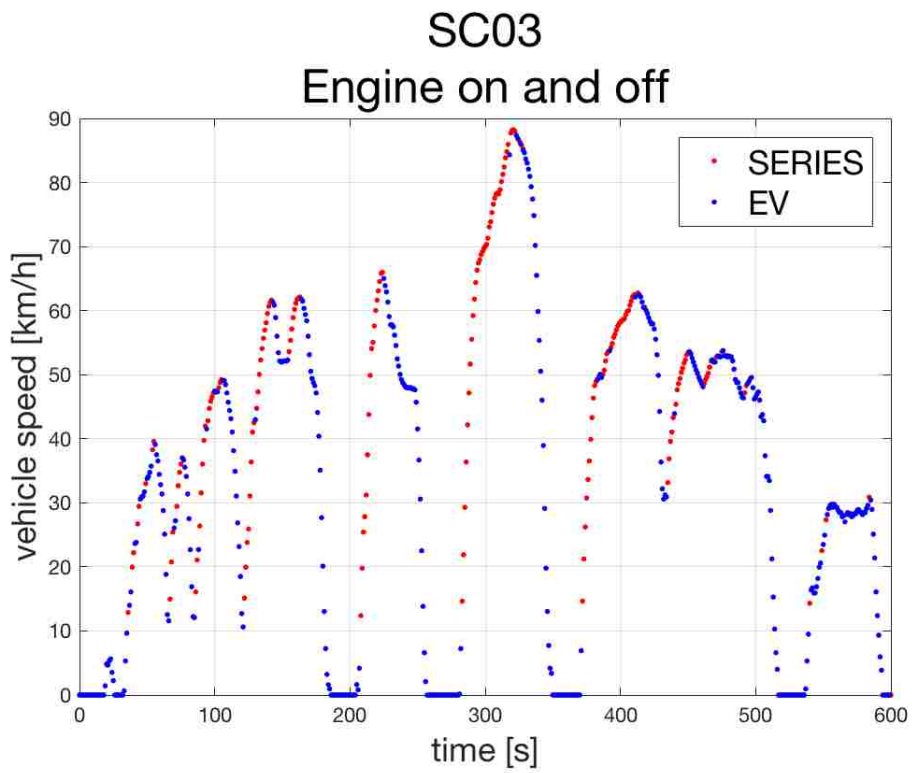


Figure 4.20 Vehicle operating modes switching over SC03 cycle (point by point)

4.2.5 NYCC

The time length and distance of NYCC are 598 seconds and 1.9 kilometers.

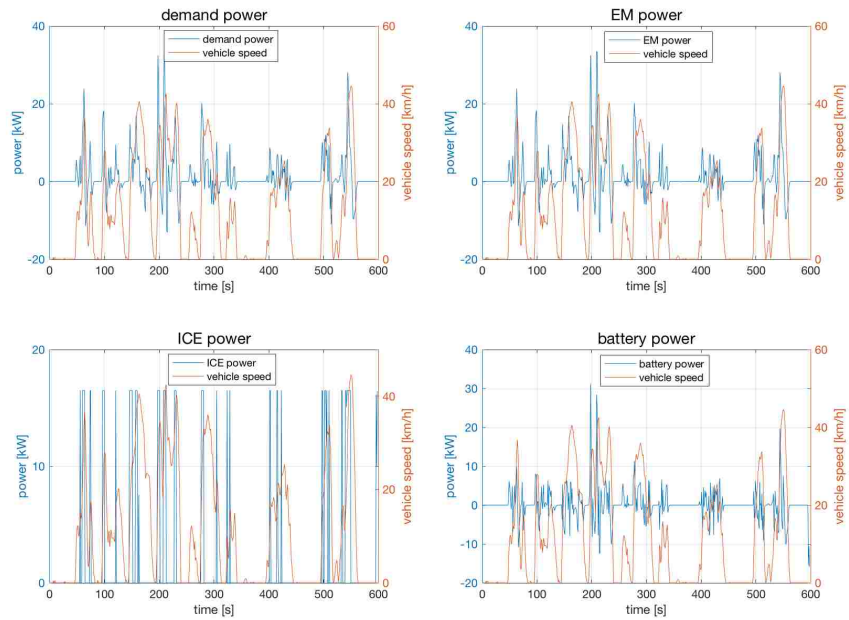


Figure 4.21 Results for demand power, EM power, ICE power, and battery power for NYCC

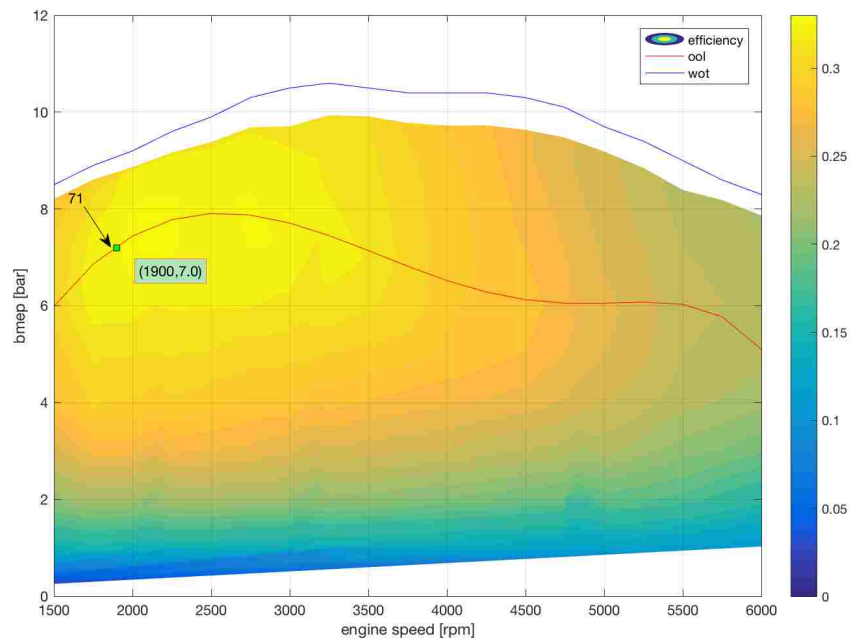


Figure 4.22 Optimal operating line and full load line for NYCC

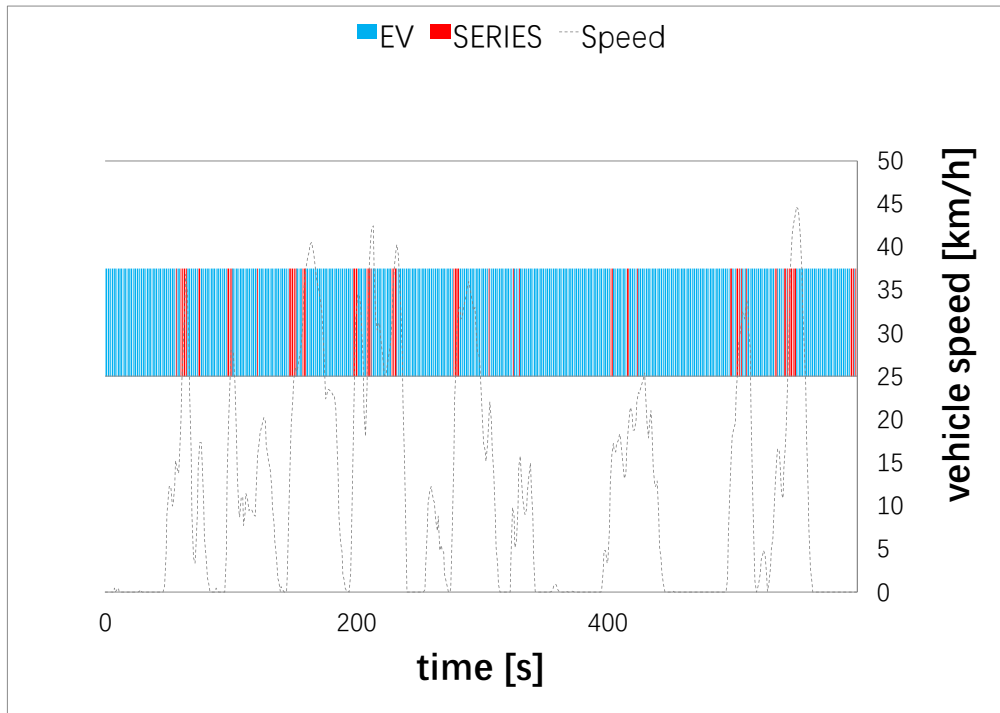


Figure 4.23 Vehicle operating modes switching over NYCC

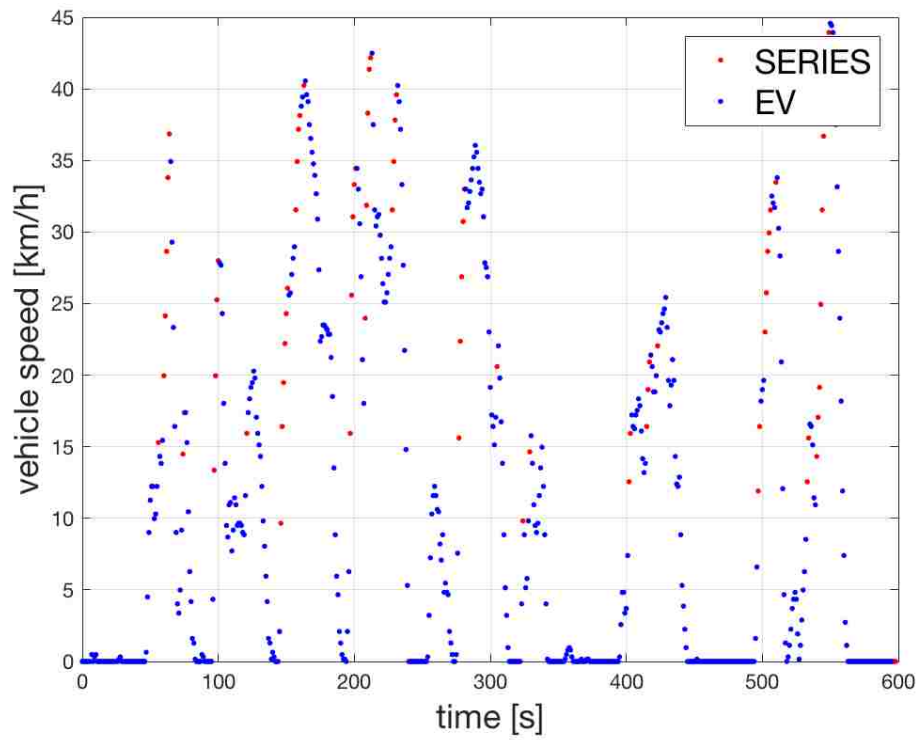


Figure 4.24 Vehicle operating modes switching over NYCC (point by point)

4.2.6 HWFET

The time length and distance of HWFET are 765 seconds and 16.5 kilometers.

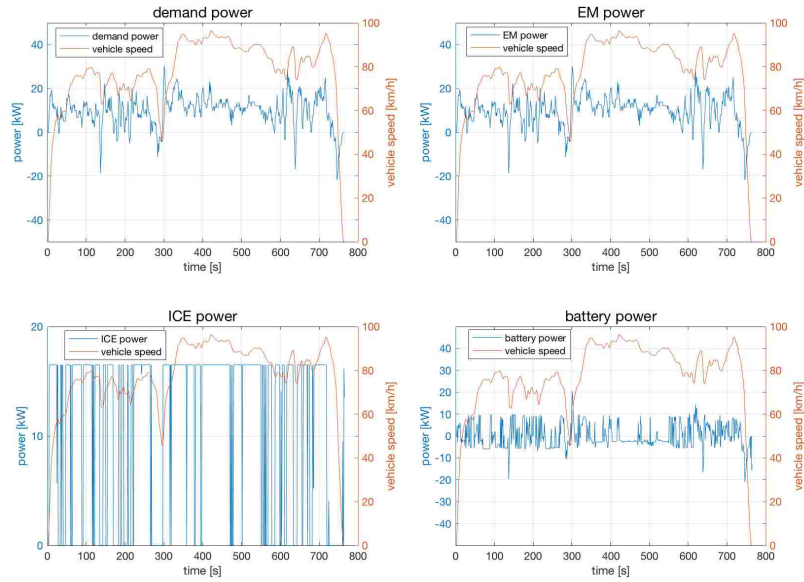


Figure 4.25 Results for demand power, EM power, ICE power, and battery power for HWFET cycle

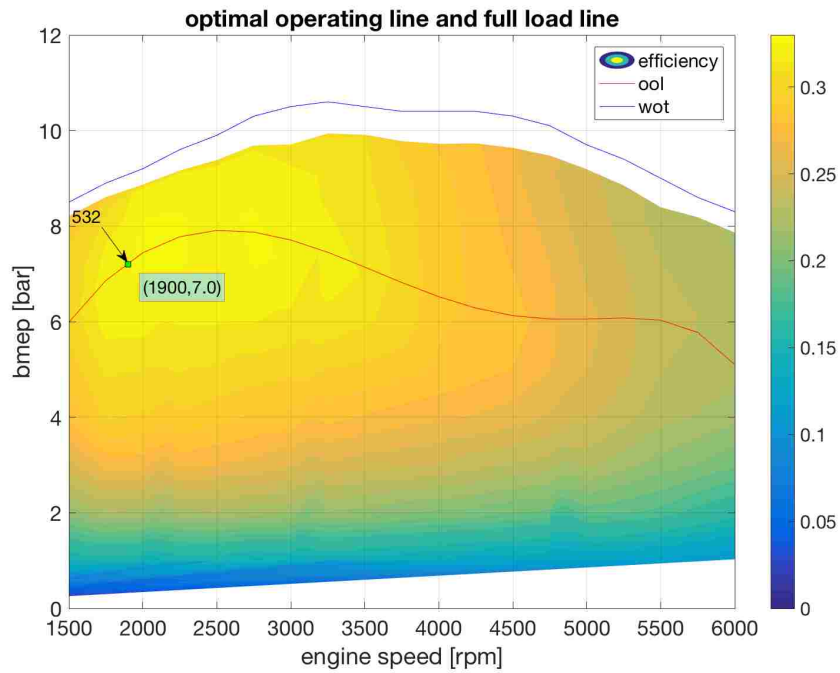


Figure 4.26 Optimal operating line and full load line for HWFET cycle

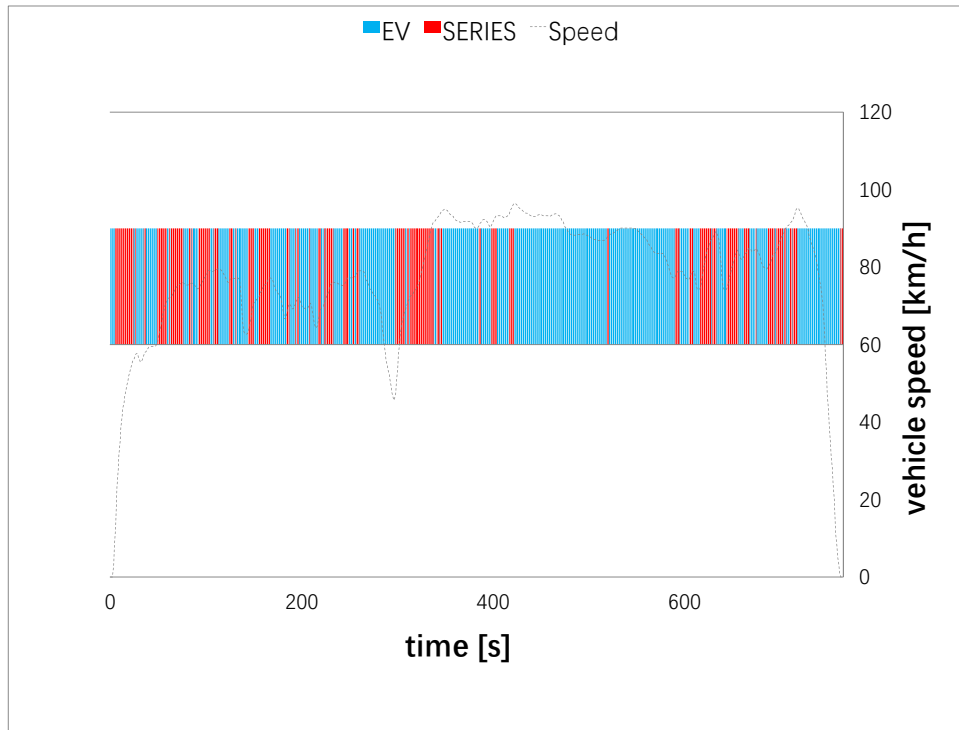


Figure 4.27 Vehicle operating modes switching over HWFET cycle

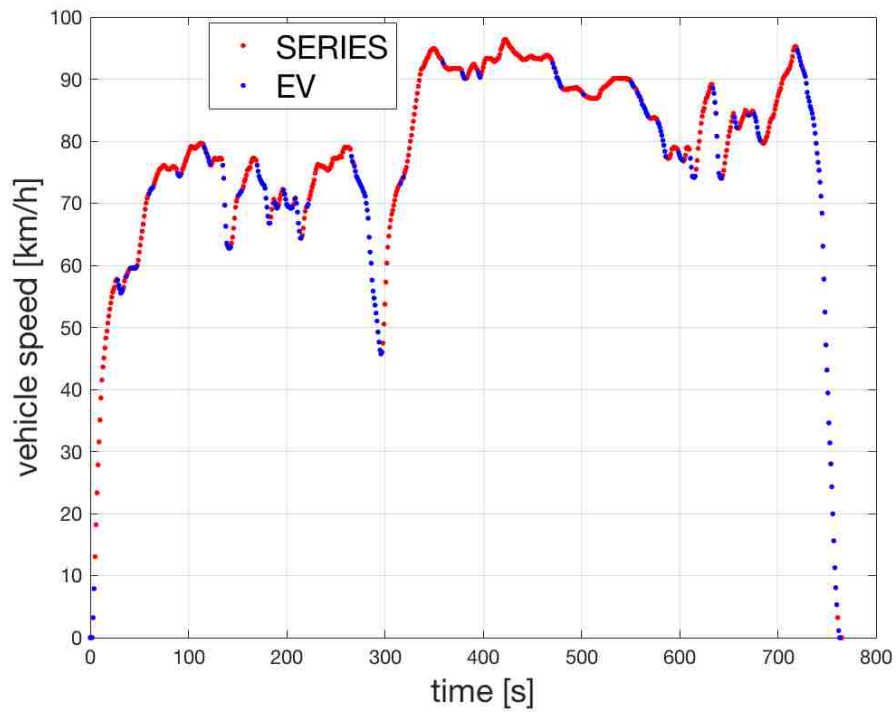


Figure 4.28 Vehicle operating modes switching over HWFET cycle (point by point)

4.2.7 FTP75

The time length and distance of FTP75 are 1874 seconds and 17.77 kilometers.

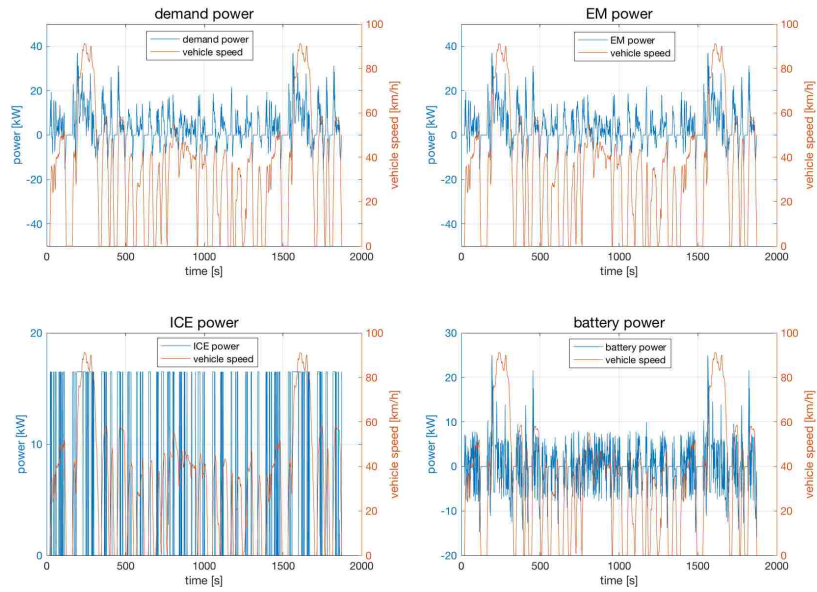


Figure 4.29 Results for demand power, EM power, ICE power, and battery power for FTP75 cycle

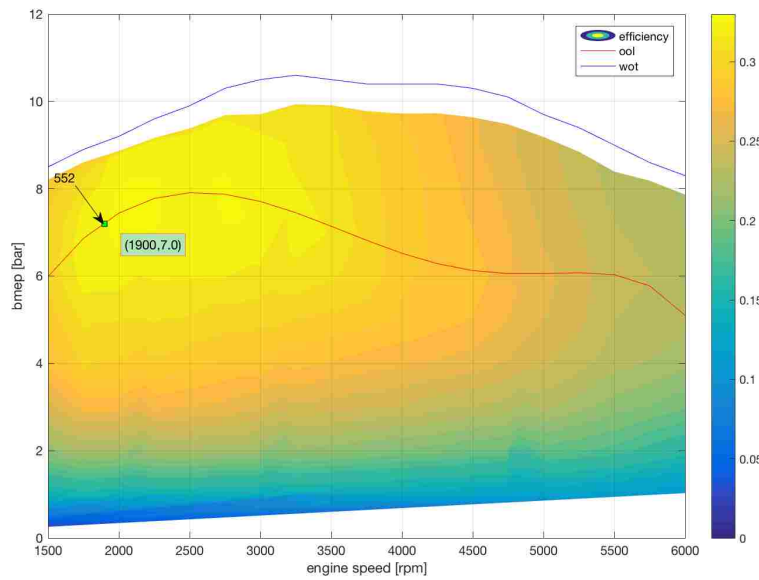


Figure 4.30 Optimal operating line and full load line for FTP75 cycle

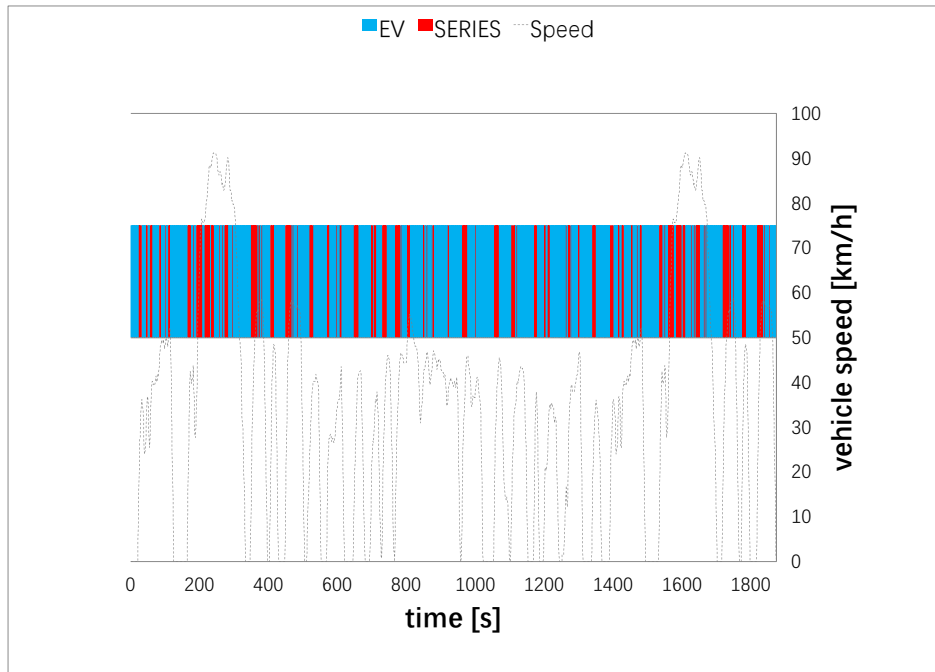


Figure 4.31 Vehicle operating modes switching over FTP75 cycle

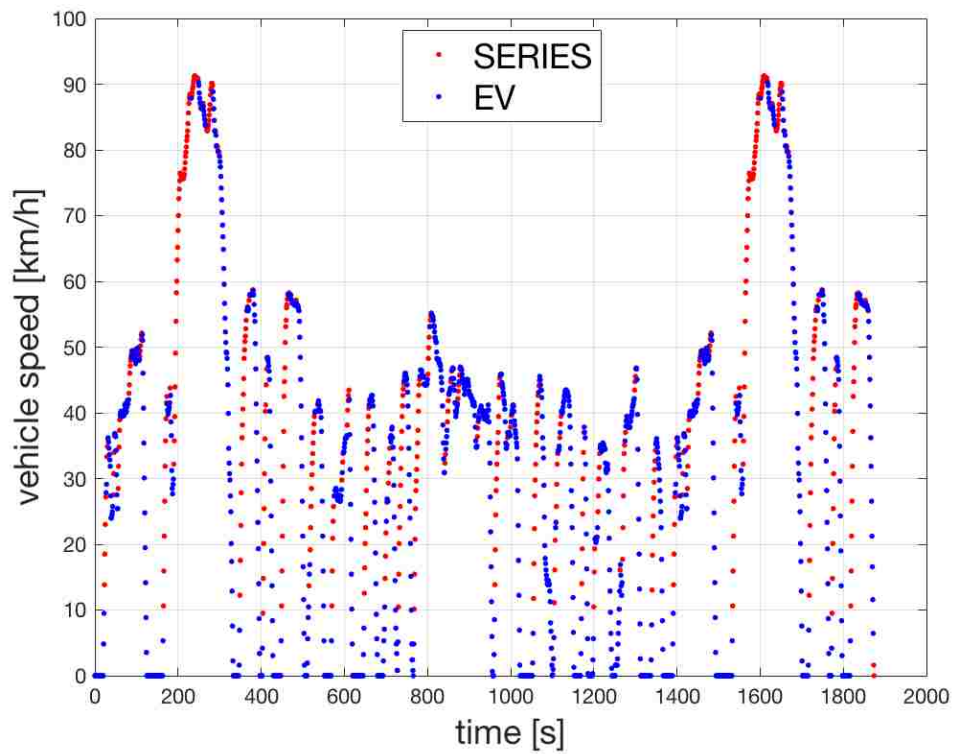


Figure 4.32 Vehicle operating modes switching over FTP75 (point by point)

4.2.8 Summary of Driving cycles

Figure 4.33 shows the variations of SOC along different driving cycles, all of them are bounded between 0.28 and 0.32 as prescribed in DP section.

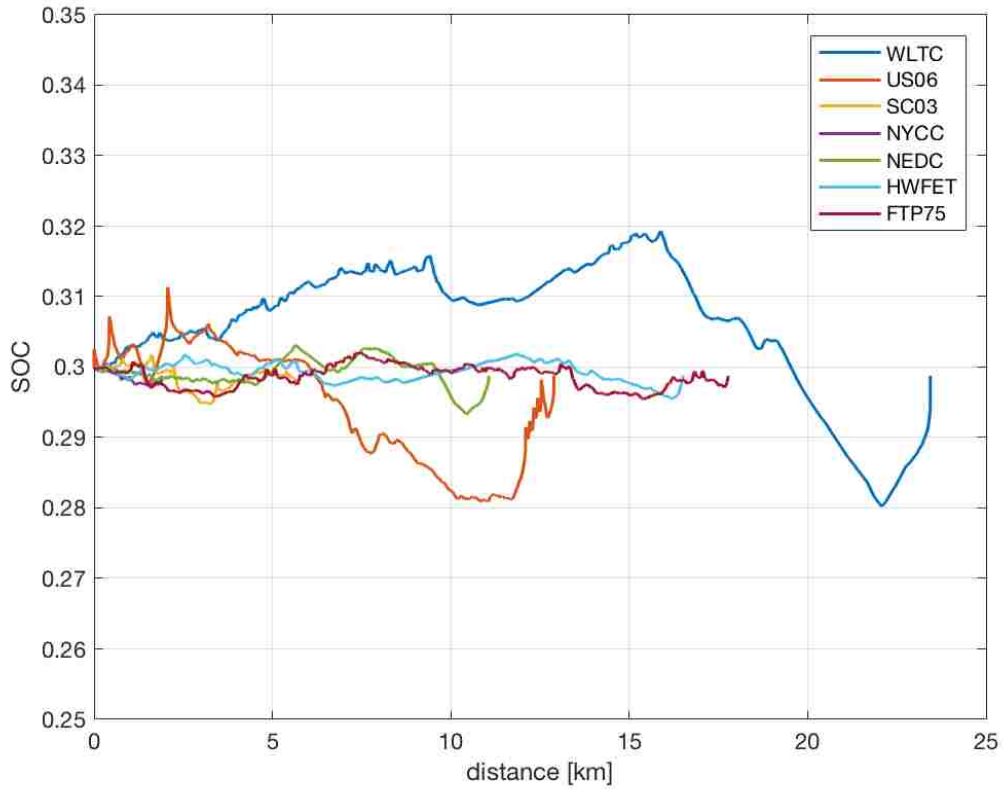


Figure 4.33 Variations of SOC along different driving cycles

In Table 4.7, results of the CO₂ production over different driving cycles are summarized. The part from the battery is negligible, since the vehicle runs in charge sustaining mode, in which case the variation of SOC is considerably small. The emission of CO₂ varies from its minimum value of 100.3 g/km for NEDC to its maximum value of 186.3 g/km for US06.

$P_{AUX} = 0 \text{ W}$	
Driving cycle	CO2 production [g/km]
NEDC	100.3
WLTC	139.8
SC03	120.2
US06	186.3
HWFET	119.4
FTP75	114.7
NYCC	144.9

Table 4.7 Results of CO2 production over different driving cycles

4.2.9 Effect of Auxiliary Power

Again, the effect of auxiliary power on CO2 production is explored over all driving cycles. The results are shown in the Tables 4.8, 4.9, 4.10, and 4.11.

$P_{AUX} = 500 \text{ W}$	
Driving cycle	CO2 production [g/km]
NEDC	112.6
WLTC	148.9
SC03	132.3
US06	192.1
HWFET	124.7
FTP75	126.9
NYCC	181.2

Table 4.8 Effect on CO₂ production of adding auxiliary power of 500 W

$P_{AUX} = 1000 \text{ W}$	
Driving cycle	CO2 production [g/km]
NEDC	125.3
WLTC	158.1
SC03	144.4
US06	197.9
HWFET	130.0
FTP75	139.0
NYCC	219.1

Table 4.9 Effect on CO₂ production of adding auxiliary power of 1000 W

$P_{AUX} = 1500 \text{ W}$	
Driving cycle	CO2 production [g/km]
NEDC	138.1
WLTC	167.2
SC03	156.9
US06	203.6
HWFET	135.2
FTP75	151.2
NYCC	254.8

Table 4.10 Effect on CO₂ production of adding auxiliary power of 1500 W

$P_{AUX} = 2000 \text{ W}$	
Driving cycle	CO2 production [g/km]
NEDC	151.1
WLTC	177.0
SC03	168.6
US06	209.4
HWFET	140.6
FTP75	163.5
NYCC	291.7

Table 4.11 Effect on CO₂ production of adding auxiliary power of 2000 W

Figure 4.34 illustrates that CO₂ emission will increase as the auxiliary power rises. Table 4.12 lists the mean demand power over all the driving cycles. The higher the mean demand power is, the less the effect of the added auxiliary power on the amount of CO₂ emission is.

It can be seen from Figure 4.34 that the CO₂ production for NYCC increases dramatically with the increment of auxiliary power, because there are a lot of accelerations and the added auxiliary power adds a lot to the overall demand power for NYCC as shown in Table 4.12. With regard to SC03, the emission of carbon dioxide remains at a relatively high value, compared to all the other driving cycles, and it is not influenced a lot by the increment of the auxiliary power. Moreover, among all the driving cycles, the CO₂ emission for NEDC is the lowest, but it overtakes that of HWFET when 1500 W of auxiliary power is added. In terms of HWFET, the CO₂ emission remains at a comparatively low level and the increased auxiliary power does not influence much the amount of CO₂ emission.

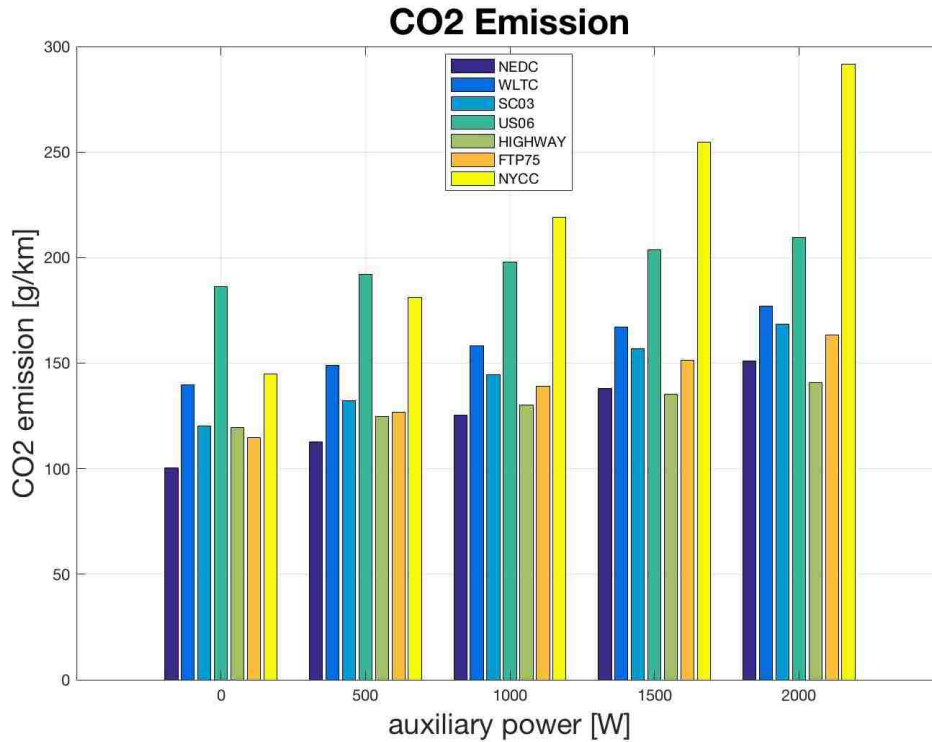


Figure 4.34 Results of sensitivity analysis on CO₂ emission

Mean value of demand power [kW]	
NYCC	1.4
NEDC	3.1
FTP75	3.8
SC03	3.9
WLTC	6.5
HIGHWAY	9.6
US06	14

Table 4.12 Mean value of demand power over different driving cycles

4.3 Rules Extraction

The minimum value of CO₂ emission over a certain range with a certain powertrain can always be found with the application of dynamic programming. However, dynamic programming itself cannot be applied in a vehicle control unit, since it requires a-priori knowledge of the driving

cycle. Nevertheless, DP results are still available for extracting rules in which suitable thresholds (power, vehicle speed, acceleration) are identified for a rule-based control strategy

4.3.1 Threshold of demand power

To avoid the ICE from frequently turning on and off, both a lower and an upper threshold of demand power will be selected. For the lower one, it is set to 0 W, because it is normal that a HEV in SERIES mode is never enabled during stops and cut-off phases.

Regarding the upper demand power threshold, it is derived by analyzing the dynamic programming results. Figure 4.35 presents the number of points in SERIES and EV modes in terms of demand power. An initial guess of 5 kW of the upper threshold of demand power is made.

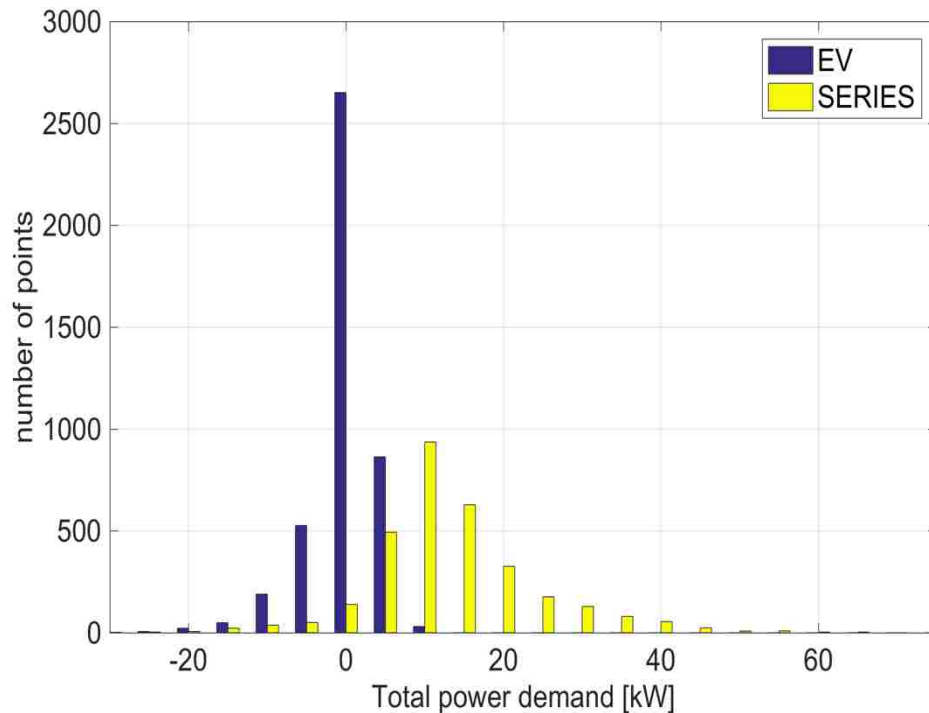


Figure 4.35 Number of points for EV and SERIES modes for each demand power

The line of upper threshold is drawn in Figure 4.36, and it separates the two areas of EV and SERIES modes. Afterwards, a simple calculation was made by trying the values nearby 5 kW (4-6 kW with a step of 0.5 kW) and counting the points in EV or SERIES mode.

Upper Threshold of demand power [kW]	Percentage of points above (EV mode) and below (SERIES mode) the upper threshold	
	EV	SERIES
4	11%	9%
4.5	9%	9%
5	6%	10%
5.5	5%	12%
6	3%	15%

Table 4.13 Percentage of points outside the upper threshold for both EV and SERIES mode for different demand power

Therefore, 4.5 kW is considered as the best compromise value, because both the percentages of the EV and SERIES points excluded by the proposed upper threshold are equal and relatively minimal.

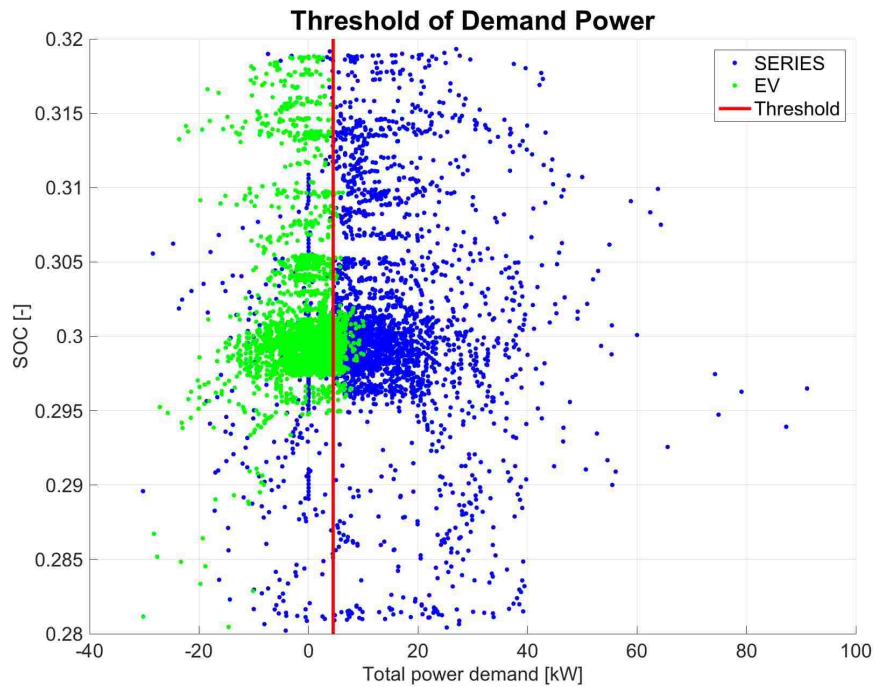


Figure 4.36 Upper threshold of demand power

Figures 4.37 and 4.38 graphically show the distribution of EV and SERIES points excluded by the determined upper demand power threshold.

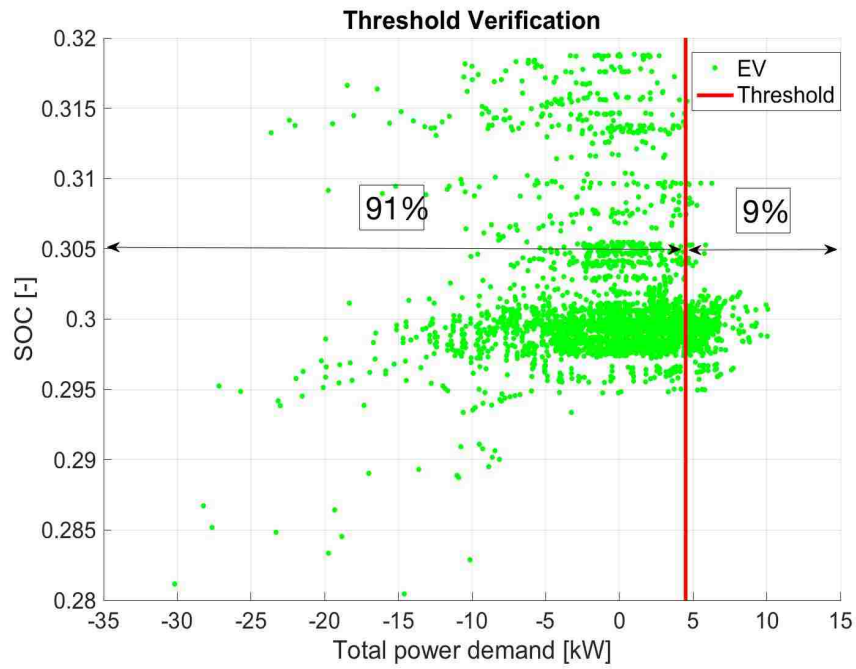


Figure 4.37 Upper threshold verification for EV mode

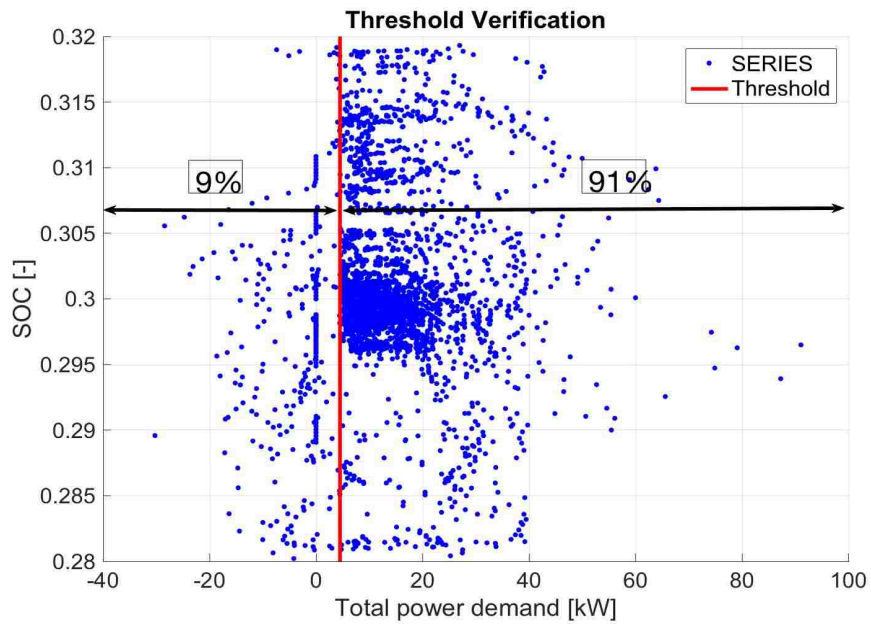


Figure 4.38 Upper threshold verification for SERIES mode

To conclude, the upper and lower thresholds of demand power were determined as 4.5 kW and 0 kW respectively.

4.3.2 Threshold of vehicle speed

In terms of vehicle speed, there is not a clear boundary as occurred in the case of the demand power as shown in Figure 4.39. Under this circumstance, the threshold of the vehicle speed is not used, in terms of the indeterminacy. Instead, the vehicle acceleration is taken into consideration.

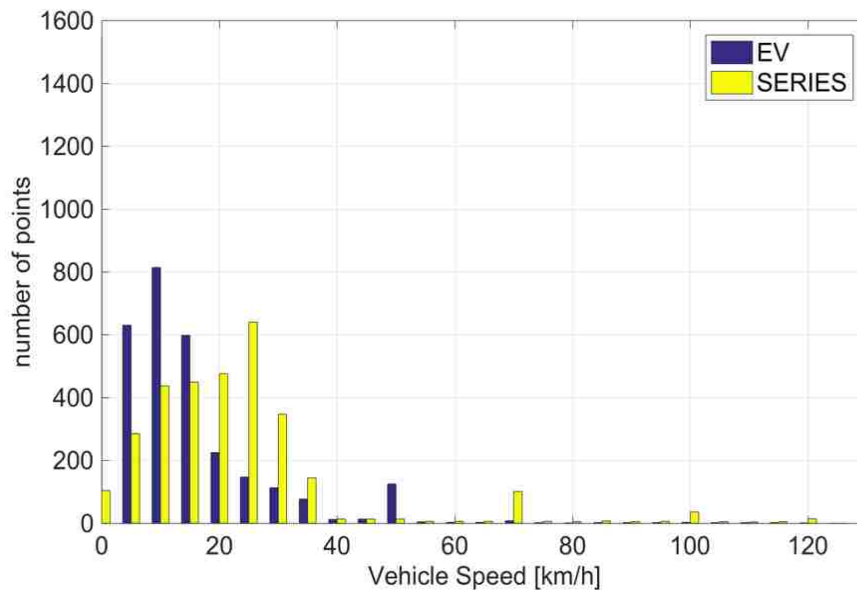


Figure 4.39 Number of points for EV and SERIES modes for different vehicle speeds

4.3.3 Threshold of vehicle acceleration

With regard to the vehicle acceleration, it is actually quite obvious from Figure 4.40 that a boundary of 0 m/s² divides the areas of the two modes. Therefore, an upper threshold was determined as 0 m/s². To avoid the ICE frequently being turned on and off, the lower threshold of acceleration was set to -1 m/s² so as to contain the overwhelming majority of the SERIES points.

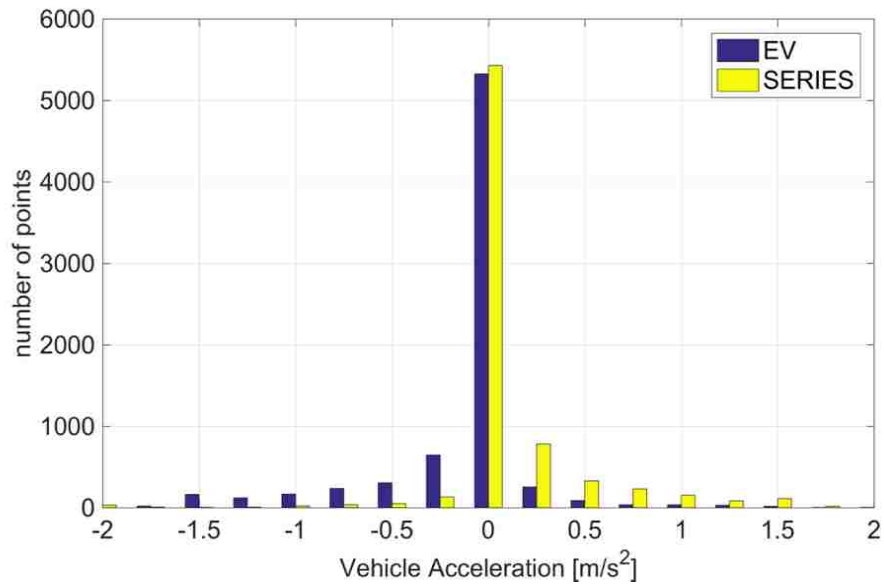


Figure 4.40 Number of points for EV and SERIES modes for each vehicle acceleration

The upper threshold is drawn in Figure 4.41, which separates the areas of EV and SERIES modes.

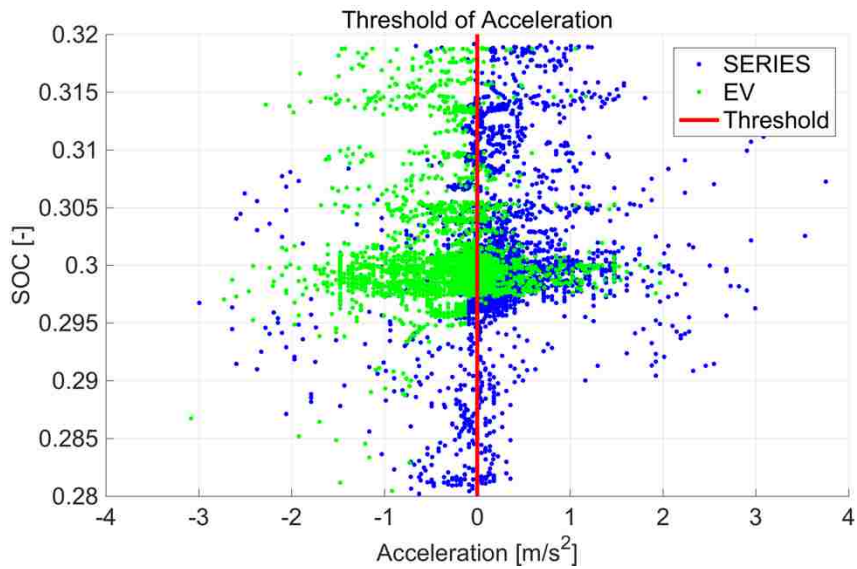


Figure 4.41 Upper threshold of vehicle acceleration

Figures 4.42 and 4.43 show that the percentages of EV and SERIES points outside the determined upper threshold are 18% and 20 % respectively.

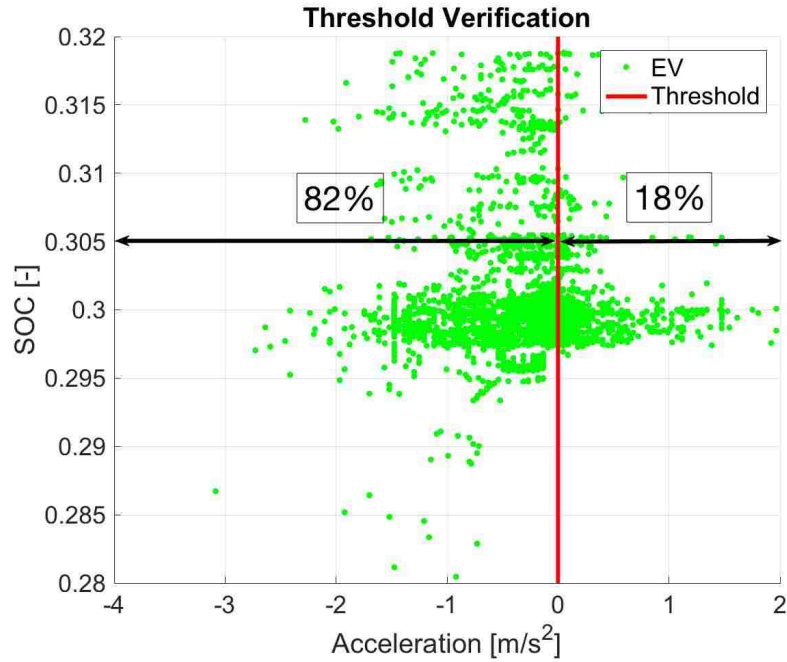


Figure 4.42 Upper Acceleration threshold verification for EV mode

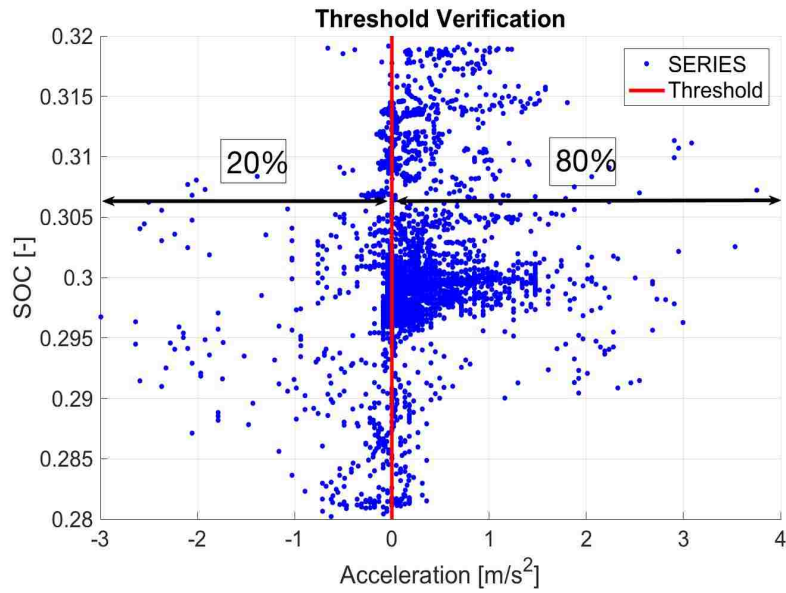


Figure 4.43 Upper Acceleration threshold verification for SERIES mode

To summarize, the upper and lower thresholds of vehicle acceleration are 0 m/s^2 and -1 m/s^2 .

4.3.4 Proposed Rule-based Control Strategy

In addition to the thresholds determined above, the variation of SOC is also taken into consideration, which is supposed to be within the range from 0.28 to 0.32 as prescribed in the DP

section. If the SOC goes below 0.28, the SERIES mode is enabled; if SOC rises above 0.32, the operation mode goes back to EV. Finally, flow charts of the rule-based control strategy are drawn in Figure 4.44. The ECU is supposed to record the state of previous time instant. If it was in EV mode, it should check if it is necessary to change from EV to SERIES mode according to the first flow chart. If it was in SERIES mode, the second flow chart is applied to verify the necessity of changing from SERIES mode to EV mode.

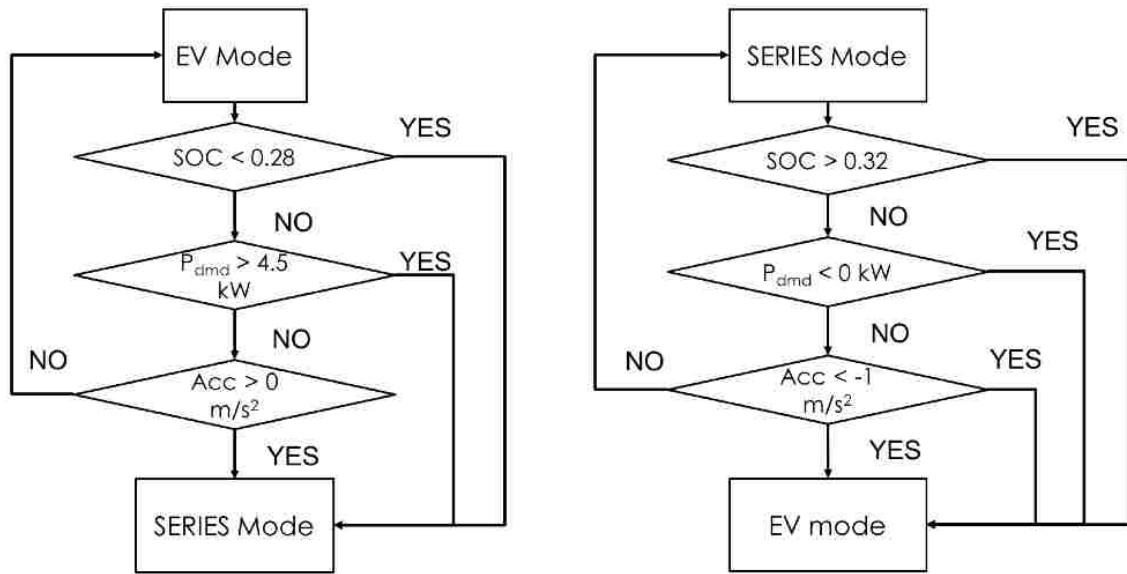


Figure 4.44 Rule-Based Control Strategy

4.3.5 Effect of auxiliary power

Table 4.14 presents the designed upper and lower thresholds of the demand power and the acceleration with different values of the auxiliary power, as well as the percentage of EV and SERIES points beyond the defined threshold. It can be seen that the upper threshold of demand power decreases, as the auxiliary power rises, since the total energy consumption goes up and the ICE is turned on more frequently to charge the battery. For the threshold of acceleration, it remains the same, but the percentage of the EV points outside the threshold is getting smaller.

The designed control strategy was applied to the obtained DP results. For every point, its state of ‘EV’ or ‘SERIES’ mode is redefined according to the developed rule-based control algorithm. The differences between the old and new numbers of EV and SERIES points were computed. The results are presented in the last column of Table 4.14.

Proposed Rule-based Control Strategy										
Auxiliary power [W]	Demand Power				Acceleration				Overall	
	Upper Threshold [kW]	Lower Threshold [kW]	% of outside points		Upper Threshold [m/s ²]	Lower Threshold [m/s ²]	% of outside points		Difference with DP in percentage	
			EV	SERIES			EV	SERIES	EV	SERIES
0	4.5	0	9%	9%	0	-1	18%	20%	17%	24%
500	4	0	7%	9%	0	-1	16%	20%	14%	17%
1000	3	0	9%	9%	0	-1	13%	20%	11%	13%
1500	2.5	0	9%	9%	0	-1	10%	20%	9%	9%
2000	2	0	10%	8%	0	-1	8%	21%	7%	6%

Table 4.14 Effect of auxiliary power on the thresholds

5 CONCLUSIONS AND RECOMMENDATIONS

5.1 Conclusions

With the motivation of mitigating the greenhouse effect due to automobiles and meeting the increasingly strict regulations on CO₂ emissions around the world, in this thesis, a R-EX model was established to evaluate the minimum CO₂ emission over different standard driving cycles by applying the dynamic programming function. From these results, a feasible rule-based control strategy was developed through rules extraction. Seven driving cycles were used to enrich the potential situations that a vehicle may come across in a real driving condition.

The electric range and energy consumption vary according to different demanding road conditions. The electric range can reach at maximum 100 km for the least demanding driving cycle of NEDC, while the energy consumption is 11.5 kWh /100 km. The effects of the added auxiliary power on both the electric range and energy consumption are significant; for example, the electric range of WLTC decreases from 70.3 km to 40.6 km and the energy consumption increases from 176.5 Wh/ km to 187.3 Wh/km with an additional auxiliary power of 500 W. It leads to a conclusion that potential benefits could be obtained from by improving the management strategy of the auxiliary devices. The evaluation of the effect of carbon intensity of electricity shows the advantage in terms of reducing CO₂ emission by altering the energy sources from natural gas to electricity; however, it also reflects the limitation for HEVs of reducing CO₂ emission in some developing countries.

The dynamic programming has been demonstrated to be an effective mean of determining the optimal path that gives the minimum CO₂ emission. From DP results, the optimal engine operating points are also calculated in terms of different driving cycles according to the engine efficiency map. For most of the driving cycles, the operating point is located at engine speed 2000 rpm and bmep 7.5 bar with 16.5 kW. The influence of the auxiliary power is distinct on the CO₂ emission and it correlates to the demanding conditions for different driving cycles. The higher the mean demand power is, the less the effect of the increased auxiliary power on the amount of CO₂ emission is.

The proposed rule based control strategy from the case study is a feasible option that is implementable for an electrical control unit. The threshold of acceleration is constant in terms of

the increment of the auxiliary power; regarding the demanding power, it is adjusted to the rise of auxiliary power. The threshold of vehicle speed is not applied considering the indeterminacy of its effect. The comparison of state of points between the proposed methodology with the dynamic programming result shows effectiveness of the proposed algorithm, however, further investigation must be done in order to evaluate the difference of CO₂ emission.

5.2 Recommendations

The proposed rule-based control strategy cannot be evaluated with MATLAB, since setting up a simulation model which is able to correctly simulate the operation of a PHEV or of a RE-EV with a rule-based strategy is quite complex. The test of a rule-based strategy usually uses complex models built in GT-Suite. In this case, the evaluation of the proposed rule-based control strategy is the first future work. The threshold of vehicle speed can also be evaluated by setting different values during the simulation.

From the simulation results, while the vehicle is running in charge sustaining condition, even the minimum CO₂ emission cannot meet the stringent regulation of automobile CO₂ production of 95 g/km in Europe by 2020. Therefore, the efficiency of the engine is an important factor for the decrement of CO₂ emission. A potential method of improving the control strategy is to change the size or the type of the engine. The 1.4 L spark ignition (SI) engine could be replaced by a 0.6 L SI engine to evaluate the effect of downsizing of the engine. A diesel engine could be taken into consideration, since it has higher combustion efficiency compared to a gasoline engine with the same size.

Moreover, the vehicle model can also be improved by introducing quasi-static approach or dynamic approach, which are capable of simulating transient conditions to give more accurate simulation results. The effect of the temperature on modelling the battery, the electric machines can be investigated. The delay time of starting the engine is also influenced by the engine coolant temperature.

All in all, the thesis has introduced a valuable method to develop a power management strategy of a range extended hybrid electric vehicle. There are still many improvements to be applied in terms of the modeling approach and the design of the control strategy to meet different

requirements. The goal of the optimization can also be altered to the vehicle performance or the fuel economy.

REFERENCES

- [1] *January 2014 EU CO₂ Emission Standards for Passenger Cars and Light-Commercial Vehicles*, (2014, January). Retrieved from http://www.theicct.org/sites/default/files/publications/ICCTupdate_EU-95gram_jan2014.pdf
- [2] *Reducing CO₂ emissions from passenger car*, (2015). Retrieved from https://ec.europa.eu/clima/policies/transport/vehicles/cars_en
- [3] *Hybrid electric vehicle*, (2017 March). Retrieved from https://en.wikipedia.org/wiki/Hybrid_electric_vehicle
- [4] *Clean vehicles/Electric vehicle/Average emission nationwide* (2017). Retrieved from http://www.ucsusa.org/clean-vehicles/electric-vehicles/ev-emissions-tool#z/NATIONAL/_/_/
- [5] Federico Millo, Luciano Rolando, Fabio Mallamo and Rocco Fuso, *Development of an optimal strategy for the energy management of a range-extended electric vehicle with additional noise, vibration and harshness constraints*, 12 October 2012. *Proceedings of the Institution of Mechanical Engineers, Part D: Journal of Automobile Engineering* published online 12 October 2012 DOI: 10.1177/0954407012457488
- [6] Serrao, L., Onori, S., and Rizzoni, G.: *A comparative analysis of energy management strategies for hybrid electric vehicles*, *Journal of Dynamic Systems, Measurement and Control* (ASME), May 2011
- [7] Sebastiano La Ferla *Development of an energy management strategy for a series hybrid electric vehicle: COMFORT mode*. Politecnico di Torino, Master of Science in Automotive Engineering, March 2016
- [8] *Sensitivity analysis*. Retrieved from https://en.wikipedia.org/wiki/Sensitivity_analysis
- [9] Federico Millo, Luciano Rolando, Rocco Fuso, Fabio Mallamo, *Real CO₂ emissions benefits and end user's operating costs of a plug-in Hybrid Electric Vehicle*, *Science Direct, Applied Energy* 114(2014) 563-571. 14 September. 2014
- [10] Olle Sundstrom and Lino Guzzella, *A Generic Dynamic Programming Matlab Function*, *Oil & Gas Science and Technology. Rev. IFP*, Vol. 65 (2010), No. 1, pp. 91-102, Institut français du pétrole DOI: 10.2516, February, 2009
- [11] Federico Millo, Luciano Rolando and Maurizio Andreatta, *Numerical Simulation for Vehicle Powertrain Development*. September 9, 2011. Retrieved from <https://www.intechopen.com/books/numerical-analysis-theory-and-application/numerical-simulation-for-vehicle-powertrain-development>
- [12] Rhodes, K., Kok, D., Sohoni, P., Perry, E. et al., *Estimation of the Effects of Auxiliary Electrical Loads on Hybrid Electric Vehicle Fuel Economy*, *SAE Technical Paper* 2017-01-1155, 2017
- [13] Ivan Arsie, Marco Graziosi, Cesare Pianese, Gianfranco Rizzo, Marco Sorrentino, *Optimization of supervisory control strategy for parallel hybrid vehicle with provisional load estimate*. Retrieved from https://www.researchgate.net/publication/228806335_Optimization_of_supervisory_control_strategy_for_parallel_hybrid_vehicle_with_provisional_load_estimate
- [14] Aymen Flah, Sbita Lassaad, Chokri Mahmoudi, *Overview of Electric Vehicle Concept and Power Management Strategies*, November 2014. Retrieved from <https://www.researchgate.net/publication/265709143>
- [15] Chih-Wei Hung, Tri-Vien Vu, Chih-Keng Chen. *The Development of an Optimal Control Strategy for a Series Hydraulic Hybrid Vehicle. Applied Sciences* (2076-3417). Apr2016, Vol. 6 Issue 4, p1-18. 18p
- [16] Matthew Brander, Aman Sood, Charlotte Wylie, Amy Houghton, Jessica Lovell. *Electricity-specific emission factors for grid electricity*. Retrieved from <https://ecometrica.com/assets/Electricity-specific-emission-factors-for-grid-electricity.pdf>
- [17] *Fuel cell vehicle*. Retrieved from https://en.wikipedia.org/wiki/Fuel_cell_vehicle

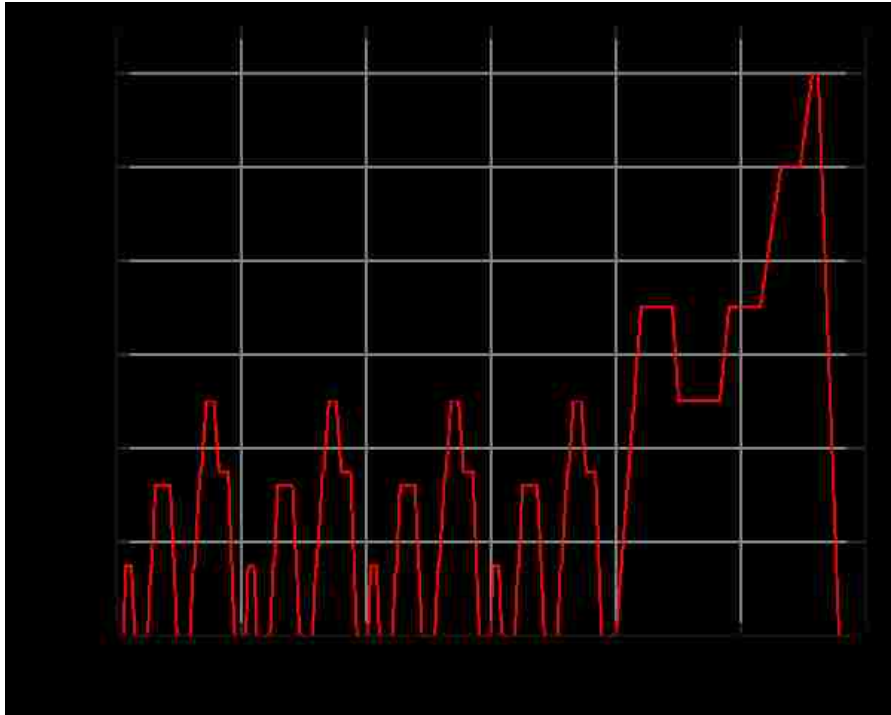
- [18] Hong Huo, *Environmental Implication of Electric Vehicle in China*. Environ. Sci. Technol., **2010**, 44 (13), pp 4856–4861 24 May, 2010
- [19] Chan-Chiao Lin, Jun-Mo Kang, J.W. Grizzle, Huei Peng, *Energy Management Strategy for a Parallel Hybrid Electric Truck*. Proceedings of the American Control Conference Arlington, VA June 25-27, 2001
- [20] G-Q Ao, J-X Qiang, H Zhong, X-J Mao, L Yang, B Zhuo *Fuel economy and NO_x emission potential investigation and trade-off of a hybrid electric vehicle based on dynamic programming*. Retrieved from <http://journals.sagepub.com/doi/pdf/10.1243/09544070JAUTO644>
- [21] Stephan Zentner, Jonas Asprien, Christopher Onder, Lino Guzzella, *An Equivalent Emission Minimization Strategy for Causal Optimal Control of Diesel Engines*. Energies 2014, 7, 1230-1250; doi:10.3390/en7031230
- [22] Marco Sorrentino, Gianfranco Rizzo, Ivan Arsie, *Analysis of a rule-based control strategy for on-board energy management of series hybrid vehicles*, 26 August 2011
- [23] A. A. Malikopoulos, *Real-Time, Self-Learning Identification and Stochastic Optimal Control of Advanced Powertrain Systems*. Ann Arbor, MI, USA: ProQuest, Sep. 2011.
- [24] Scott J. Moura *Plug-in Hybrid Electric Vehicle Power Management: Optimal Control and Battery Sizing*. Retrieved from https://ecal.berkeley.edu/pubs/Moura_MSThesis.pdf
- [25] P. B. Sharer, A. Rousseau, D. Karbowski, and S. Pagerit, *Plug-in hybrid electric vehicle control strategy: Comparison between ev and charge-depleting options*, SAE Papers, 2008 SAE World Congress, vol. 2008-01-0460, 2008.
- [26] T. Markel and A. Simpson, *Energy storage systems considerations for grid-charged hybrid electric vehicles*. Vehicle Power and Propulsion, 2005 IEEE Conference, Chicago, IL, USA
- [27] A. F. Burke, *Batteries and ultracapacitors for electric, hybrid, and fuel cell vehicles*,” Proceedings of the IEEE, vol. 95, no. 4, pp. 806–20, 04 2007.
- [28] P. B. Sharer, A. Rousseau, S. Pagerit, and P. Nelson, *Midsized and SUV vehicle simulation results for plug-in HEV component requirements*, SAE Papers, 2007 SAE World Congress, vol. 2007-01-0295, 2007.
- [29] Chaoying Xia, Cong Zhang, *Power Management Strategy of Hybrid Electric Vehicles Based on Quadratic Performance Index*, Energies 2015, 8(11), 12458-12473; doi:10.3390/en81112325
- [30] Vibin Jacob, *Dyno theory (chassis dynamometer) and road load equation*. Retrieved from <https://www.linkedin.com/pulse/dyno-theory-chassis-dynamometer-road-load-equation-vibin-jacob>
- [31] Emma Raszmann, *Modeling Stationary Lithium-Ion Batteries for Optimization and Predictive Control*, IEEE Power and Energy Conference Champaign, Illinois February 23–24, 2017
- [32] *Regenerative brake*. Retrieved from https://en.wikipedia.org/wiki/Regenerative_brake
- [33] Marco Fogliarino, *Crankcase pressure control in an internal combustion engine: GT-Power simulation*. Politecnico di Torino, Master of Science of Automotive Engineering, 2014
- [34] *Regulation No.83*. Retrieved from <https://www.unece.org/fileadmin/DAM/trans/main/wp29/wp29regs/r083r4e.pdf>
- [35] Bertsekas, D.P. *Lecture slides on dynamic programming. Lectures, Massachusetts, Institute of Technology, Cambridge, Massachusetts, USA, 2002*
- [36] Bertsekas, D.P. *Dynamic programming and optimal control, 3rd edition*, 2005
- [37] Lorenzo Serrao, Simona Onori, Giorgio Rizzoni, *A comparative Analysis of Energy Management Strategies for Hybrid Electric Vehicles*, J. Dyn. Sys., Meas., Control 133(3), 031012 (Mar 25, 2011) (9 pages) doi:10.1115/1.4003267
- [38] Co Huynh, Liping Zheng, Dipjyoti Acharya, *Losses in High Speed Permanent Magnet Machines Used in Micro-turbine Applications*. Retrieved from <https://www.calnetix.com/sites/default/files/7.pdf>

[39] *FAQ: What are rotational losses in DC motors*. Retrieved from <http://www.motioncontroltips.com/faq-what-are-rotational-losses-in-dc-motors/>

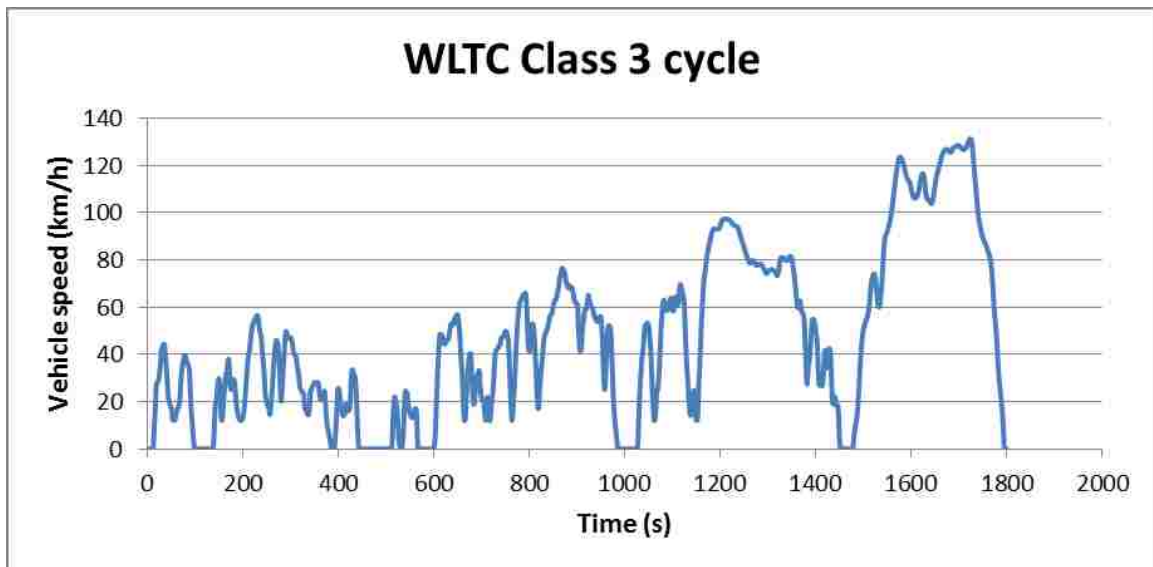
APPENDIX

Driving cycles

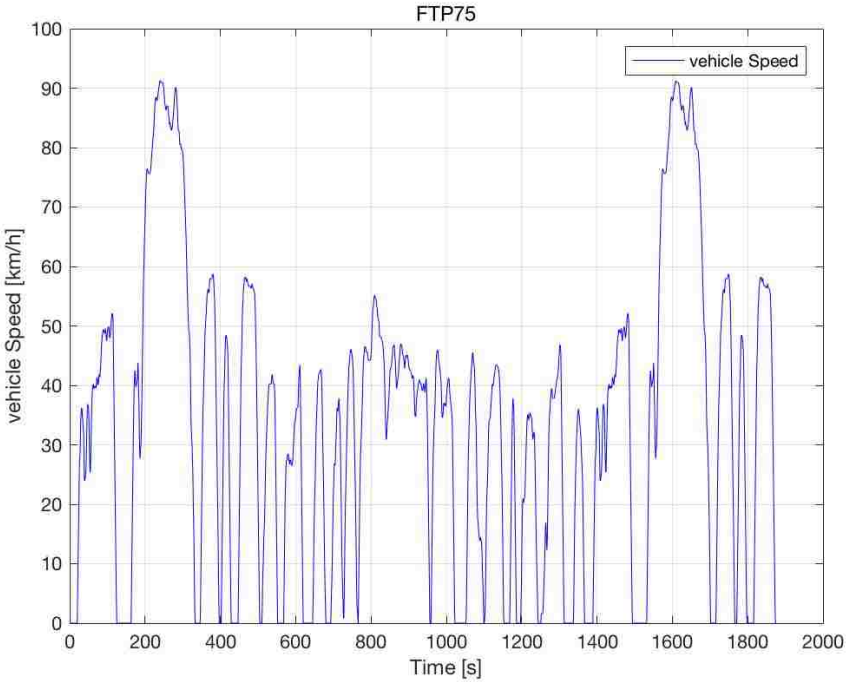
New European Driving Cycle (NEDC)



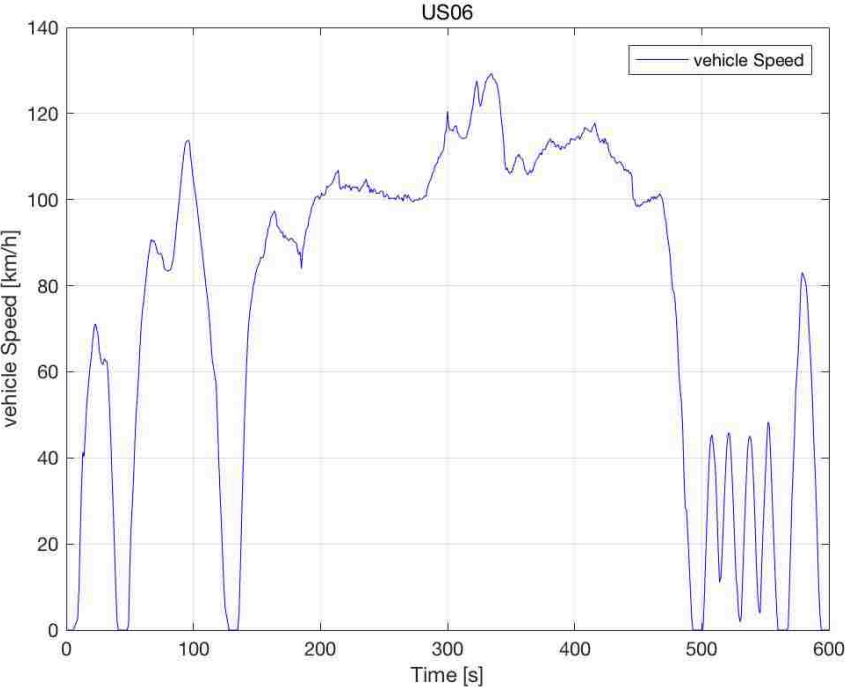
Worldwide Harmonized Light Vehicles Test Cycle (WLTC)



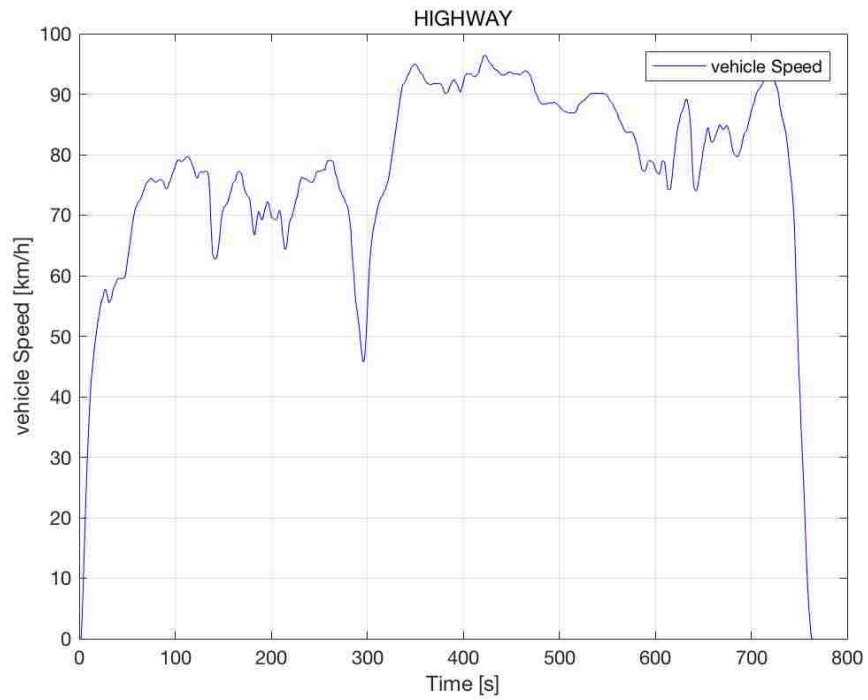
Federal Test Procedure (FTP75)



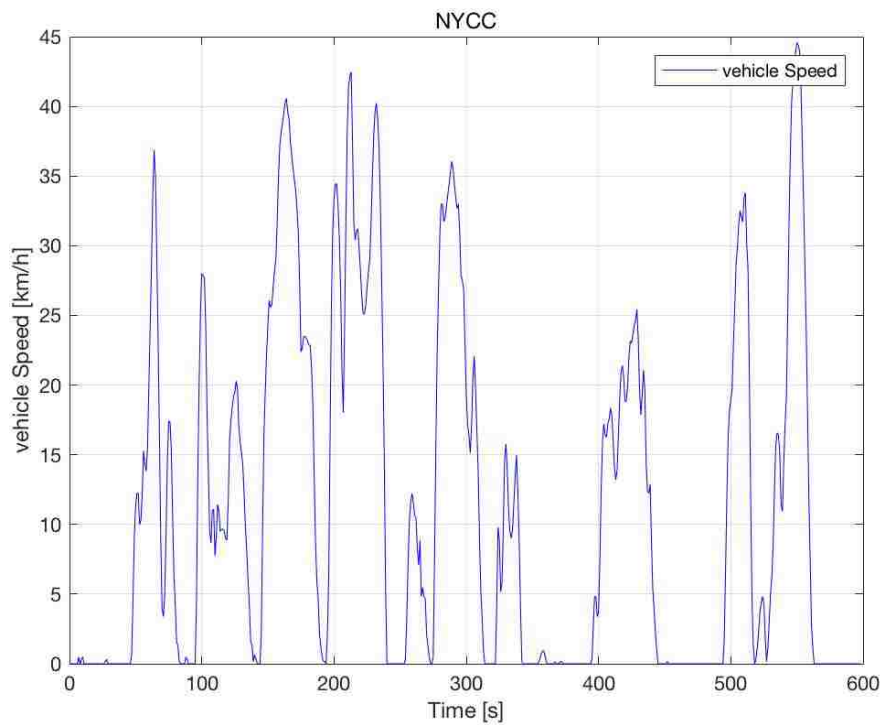
United States Supplemental Federal Test Procedure (US06)



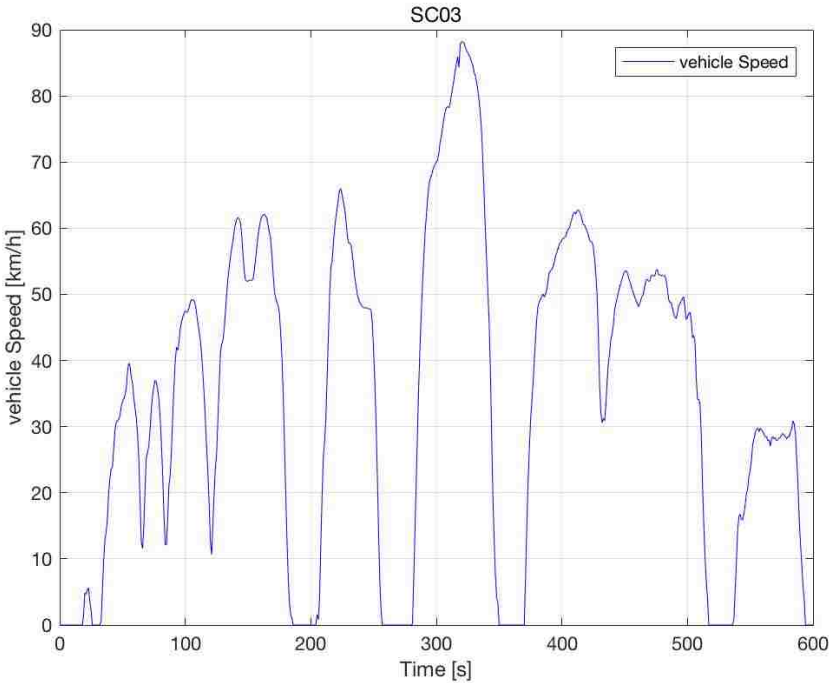
The Highway Fuel Economy Driving Schedule (HWFET)



New York City Cycle (NYCC)



Supplemental Federal Test Procedure (SC03)



VITA AUCTORIS

NAME: Wenzhou Li

PLACE OF BIRTH: Dandong, China

YEAR OF BIRTH: 1992

EDUCATION: Beijing Institute of Technology, B.Sc., Beijing, China, 2011

Politecnico di Torino, B.Sc., Turin, Italy, 2014

Politecnico di Torino, M.Sc., Turin, Italy, 2015

University of Windsor, M.Sc., Windsor, ON, 2016